

**GARY RENATO VARGAS CANALES**

**O USO DA ACÚSTICA MULTIFREQUÊNCIA NA CARACTERIZAÇÃO DAS  
COMUNIDADES PELÁGICAS EM ILHAS OCEÂNICAS DO ATLÂNTICO SUL,  
BRASIL**

**RECIFE,**

**2017**



**UNIVERSIDADE FEDERAL RURAL DE PERNAMBUCO**  
**PRÓ-REITORIA DE PESQUISA E PÓS-GRADUAÇÃO PROGRAMA DE PÓS-GRADUAÇÃO EM**  
**RECURSOS PESQUEIROS E AQUICULTURA**

**O USO DA ACÚSTICA MULTIFREQUÊNCIA NA CARACTERIZAÇÃO DAS**  
**COMUNIDADES PELÁGICAS EM ILHAS OCEÂNICAS DO ATLÂNTICO SUL,**  
**BRASIL**

**Gary Renato Vargas Canales**

Dissertação apresentada ao Programa de Pós-Graduação em Recursos Pesqueiros e Aquicultura da Universidade Federal Rural de Pernambuco como exigência para obtenção do título de Mestre.

**Prof.<sup>a</sup> Dr.<sup>a</sup> Flávia Lucena Frédou**  
Orientador

**Prof. Dr. Arnaud Bertrand**  
Co-orientador

**Recife,**  
**Fevereiro/2017**

Dados Internacionais de Catalogação na Publicação (CIP)  
Sistema Integrado de Bibliotecas da UFRPE  
Biblioteca Central, Recife-PE, Brasil

C212u Canales, Gary Renato Vargas.  
O uso da acústica multifrequência na caracterização das  
comunidades pelágicas em Ilhas Oceânicas do Atlântico Sul, Brasil  
/ Gary Renato Vargas Canales. – 2017.  
60 f.: il.

Orientadora: Flávia Lucena Frédou.  
Coorientador: Arnaud Bertrand.  
Dissertação (Mestrado) – Universidade Federal Rural de  
Pernambuco, Programa de Pós-Graduação em Recursos  
Pesqueiros e Aquicultura, Recife, BR-PE, 2017.  
Inclui referências e apêndice(s).

1. Ecos de peixes 2. Ecos de zooplâncton 3. Ecos de alga  
4. Algoritmo multifrequência 5. Fernando de Noronha I. Frédou,  
Flávia Lucena, orient. II. Bertrand, Arnaud, coorient. III. Título

CDD 639.3

**UNIVERSIDADE FEDERAL RURAL DE PERNAMBUCO**  
**PRÓ-REITORIA DE PESQUISA E PÓS-GRADUAÇÃO**  
**PROGRAMA DE PÓS-GRADUAÇÃO EM RECURSOS PESQUEIROS E AQUICULTURA**

**O USO DA ACÚSTICA MULTIFREQUÊNCIA NA CARACTERIZAÇÃO DAS  
COMUNIDADES PELÁGICAS EM ILHAS OCEÂNICAS DO ATLÂNTICO SUL,  
BRASIL**

**Gary Renato Vargas Canales**

Dissertação julgada adequada para obtenção do título de mestre em Recursos Pesqueiros e Aquicultura. Defendida e aprovada em 23/02/2017 pela seguinte Banca Examinadora.

---

**Prof.<sup>a</sup> Dr.<sup>a</sup> Flávia Lucena Frédou**

Orientadora

Departamento de Pesca/Universidade Federal Rural de Pernambuco

---

**Prof. Dr. Paulo Eurico Pires Ferreira Travassos**

Membro Interno

Departamento de Pesca/Universidade Federal Rural de Pernambuco

---

**Dr. Daniel Isaías Grados Paredes**

Membro Externo

Departamento Oceanografia/Universidade Federal de Pernambuco

## **Dedicatória**

A minha sobrinha Renata à que quero muito e  
a todas as pessoas que lutam para fazer do  
nosso mundo um lugar melhor para viver.

## **Agradecimentos**

Agradeço a Arnaud Bertrand por ter me proposto vir ao Brasil, pela sua amizade e por ter me ajudado e motivado em todos os momentos do mestrado. Sem a sua ajuda eu não teria chegado a Recife e nem terminado a dissertação.

À Professora Flavia Lucena Frédou por ter me recebido afetuosamente, por se interessar no meu trabalho e pela sua ajuda e paciência com a minha dissertação.

Aos meus amigos do laboratório *Bioimpact* que me forneceram a sua amizade e por ter me ajudado desde falar e escrever em português até com assuntos mais técnicos. Acho-me muito afortunado de pertencer à família *Bioimpact*.

À equipe de acústicos do *Institut de Recherche pour le Développement* pela sua contribuição, críticas e ideias para melhorar este trabalho

A Mariano Gutierrez, meu orientador do TCC e amigo, que foi quem motivou em mim o interesse pela acústica. Sempre ficarei grato.

Aos meus pais por todo seu amor e pelos esforços para me fornecer a educação que me permitiu seguir este caminho. Os quero muito.

Aos meus irmãos dos que tenho muitas saudades. Sempre penso em vocês.

A Sayuri por ter deixado tudo pra me acompanhar ao Brasil. Compartilhar as nossas vidas fez cada dia mais colorido.

Finalmente, mas não menos importante á CAPES pela concessão de bolsa.

## Resumo

A acústica submarina tem um potencial ainda não aproveitado no que diz respeito à caracterização da variedade de componentes bióticos dos ecossistemas. Atualmente muitos métodos (e.g., diferença da refletividade, modelos gaussianos) são usados para classificação multifrequência. Este estudo tem o objetivo de propor e implementar um método baseado na distribuição espacial multifrequência dos ecos de diferentes grupos de organismos, com aplicação em ilhas oceânicas do Nordeste do Brasil. Inicialmente, os ecos dos diferentes grupos de organismos são definidos através de amostras obtidas *in situ*. Posteriormente, aplica-se um critério de separação objetiva baseado na máxima diferença de energia acumulada em cada componente de duas frequências para maximizar a quantidade de energia dentro de cada grupo, quando comparadas com o grupo mais próximo. Este método foi aplicado usando dados coletados com quatro frequências (38, 70, 120 e 200 kHz) durante a campanha ABRAÇOS (Acoustics along the BRAzilian COaSt), no entorno do Arquipélago Fernando de Noronha (FDN) e Atol das Rocas (ADR), uma região caracterizada pela baixa produtividade e alta biodiversidade. Durante este processo, foram utilizados até cinco componentes bi-frequência. A aplicação desta metodologia permitiu a separação de 6 grupos: Peixes ( $S_{v38} \sim S_{v70} \sim S_{v120}$ ), dois tipos de Ressonantes a 38 kHz ( $S_{v38} > S_{v70} > S_{v120} > S_{v200}$ ) associados com gelatinosos, Fluid-like ( $S_{v38} < S_{v70} < S_{v120}$ ) associados com o zooplâncton, Ressonantes a 70 kHz ( $S_{v38} < S_{v70} > S_{v120} > S_{v200}$ ), associados com algas e um grupo de ecos “Não definidos”. Os resultados são coerentes em termos dos padrões de distribuição de cada um dos grupos. Pode-se observar a importância dos gelatinosos, que são o grupo dominante ao redor de FDN e ADR, formando uma densa camada sobre a termoclina. Estes resultados abrem novas possibilidades a serem exploradas acerca do conhecimento dos padrões de distribuição e interação de vários grupos biológicos em ecossistemas aquáticos.

**Palavras-chave:** ecos de peixes, ecos de zooplâncton, ecos de alga, algoritmo multifrequência, Fernando de Noronha

## Abstract

Underwater acoustics have an unrealized potential for multicomponent biotic and abiotic ecosystem characterization. A variety of methods (e.g., backscattering differences, clustering, Gaussian model) are currently used for multifrequency classification. This study aims at proposing and implementing a method based on the distribution of different groups of organisms echoes on multifrequency spatial planes, to be applied on acoustic data collected around oceanic islands of the Northeast Brazil. Initially, echoes of different groups of organism are defined a priori using *in situ* sampling. Then we apply an objective separation criteria based in the maximum difference of cumulated energy in each bi-frequency component, to maximize energy allocation within a given group when compared to the nearest one. This method was applied on four frequencies (38, 70, 120 and 200 kHz) data collected in the frame of the ABRAÇOS (Acoustics along the BRAzilian COaSt) project, around Archipelago of Fernando de Noronha and Atoll das Rocas, an area characterized by a low productivity but high biodiversity. For this process, up to five bi-frequency components were used for group discrimination. By applying the method we could discriminated six groups: Fish like ( $S_v38 \sim S_v70 \sim S_v120$ ), two types of High Resonant at 38 kHz ( $S_v38 > S_v70 > S_v120 > S_v200$ ) associated to gelatinous, Fluid Like ( $S_v38 < S_v70 < S_v120$ ) associated to crustacean macrozooplankton, High Resonant at 70 kHz ( $S_v38 < S_v70 > S_v120 > S_v200$ ) associated to algae, and a group of Unclassified echoes. Results are coherent in terms of distribution pattern of each group. Among other we could reveal the importance of gelatinous that were the dominant group in the vicinity of oceanic islands where it formed a dense layer above the thermocline. These results open new perspectives to improve knowledge on the patterns of distribution and the interaction of a variety of functional groups in this and other aquatic ecosystems.

**Key words:** fish-like, fluid-like, algae echo, multifrequency algorithm, Fernando de Noronha



## Lista de figuras

Página

Figure 1- ABRAÇOS survey track and sampling around the Archipelago of Fernando de Noronha (FDN) and Atoll das Rocas (ADR). The colors depicts the diel cycle: day in yellow, dusk in red, night in blue and dawn in cyan. Bongo stations are represented by black circles and mesopelagic trawls by black crosses. ....	20
Figure 2- Flow chart of the multifrequency method for scatter discrimination .....	21
Figure 3- Echotraces selected ( $MVBS_{38} \geq -69$ dB). Blue boxes highlight echotraces with acoustic response higher at 38 kHz than at 70 and 120 kHz (unlikely fish-echoes), the other echotraces present high and homogeneous acoustic response (typical for fish). The black line represents the seafloor.....	23
Figure 4- MVBS multifrequency response of the two groups of selected data ( $MVBS_{38} \geq -69$ dB): a) fish-like echoes and b) no fish-like echoes. ....	23
Figure 5- a) Data distribution of fish-like echoes (red points) and no fish-like echoes (blue points), the contour lines represents spatial density of the data. b) Objective separation criteria: % of energy of fish-like (red line) and no fish-like (blue line) echoes cumulated from -100 dB to -160 dB along $+MVBS_{70+120}$ . The black line shows the difference among groups; the corresponding value at X axis (-135 dB) with maximum difference defines the best limit to discriminate between the two groups. ....	24
Figure 6- a) Data distribution of fish-like echoes (red points) and no fish-like echoes (blue points), the contour lines represents spatial density of the data. b) Objective separation criteria: % of energy of fish-like (red line) and no fish-like (blue line) echoes cumulated from -25 to 10 dB along $\Delta MVBS_{70+38} + \Delta MVBS_{120+38}$ . The black line shows the difference among groups; the corresponding values at X axis (-18 dB) with maximum difference defines the best limit to discriminate between the two groups. ....	25
Figure 7- Final fish-like echograms at 38, 70 and 120 kHz. The black line represents the seafloor. ....	25
Figure 8- Echograms from Station 33, where the presence of algae was confirmed visually..	26
Figure 9- Objective separation criteria: % of energy cumulated from data selected of Station 33 (HR70) in red line and data selected of Station 06 (no HR70) in blue line from 0 to 20 dB along a) $\Delta MVBS_{70-38}$ and from -5 to 15 dB along b) $\Delta MVBS_{200-38}$ The black line shows the difference among groups; the corresponding values at X axis (8 dB for $\Delta MVBS_{70-38}$ and 2 dB	

for  $\Delta MVBS_{200-38}$ ) with maximum difference defines the best limit to discriminate between the two groups. ....27

Figure 10- Final HR70 echograms at 38, 70, 120 and 200 kHz. ....27

Figure 11- Process to discriminate Fluid like, HR38 and Unclassified. Two groups, one with a) highest MVBS at 120 or 200 kHz, another with b) highest MVBS at 38 kHz were selected and c) plotted, the contour lines represents spatial density of the data. The multidimensional objective separation criteria divided the plane in 3 regions: d) Fluid-like, e) HR38 and f) Unclassified echoes. ....28

Figure 12- Process to separate HR38 echoes. Two layers, a) the first with MVBS echoes more resonant (named HR38<sub>1</sub> in blue dashed line box) than the b) second (named HR38<sub>2</sub> in red dashed line box) at 38 kHz were extracted and a c) Objective separation criteria was performed: % of energy of HR38<sub>2</sub> (red line) and HR38<sub>1</sub> (blue line) echoes cumulated from -30 dB to -5 dB along  $\Delta MVBS_{70-38} + \Delta MVBS_{120-38}$ . The black line shows the difference among groups; the corresponding value at X axis (-17 dB) with maximum difference defines the best limit to discriminate between the two groups. Additionally, a band 1 dB thick was added between HR38<sub>1</sub> and HR38<sub>2</sub> to prevent possible overlap between them, for this reason the HR38 scatters was separated in 3 groups: d) HR38<sub>1</sub>, e) HR38<sub>2</sub> and f) the group named H38<sub>Unclassified</sub>. ....30

Figure 13- Example of synchronization between acoustic and TDR data (Station 21). The black line represents the path followed by the fishing gear during the trawl. ....31

Figure 14- Scatter plot of acoustic energy in the trawled area (in  $\log_{10} [S_{Atrawl} \cdot \text{dist}_{trawl} + 1]$ ) versus trawl catch (in  $\log_{10}[\text{Trawl catch} + 1]$ ), for (a) fish-like and (b) HR38. ....33

Figure 15- Acoustic groups detected in Stations 18 (upper panel) and 33 (middle panel), where pelagic algae presence was visually confirmed, and in Station 55 (lower panel), where no algae were present in the water column. The black line represents the bottom. ....33

Figure 16- Three dimensional distribution of the discriminated acoustics groups. ....34

Figure 17- Spatial multifrequency distribution of the different scatters classified according their  $\Delta MVBS$ . The white lines contour areas with high density of data for each group. ....34

Figure 18- Comparison between (a) an echogram (38 kHz) before, and (b) after the application of the algorithm developed for multifrequency classification. This echogram encompasses night, dawn and day periods, also illustrate a pattern of downward vertical migration between 4:45 and 7:00 hours. ....35

Figure 19- Distribution of the acoustic biomass ( $s_A$ ) of each acoustic group according to the bottom depth.....	35
Figure 20- Spatial distribution of fish-like $s_A$ at 38 kHz integrated in the first 300 m around ADR and FDN, averaged in grid size of 1 nm $\times$ 1 nm. Bottom depth contour lines in black for 100 (thick line), 300 and 500 m.....	36
Figure 21- Vertical distribution of Fish-like $s_A$ values at 38 kHz greater than zero around ADR and FDN, averaged in 10 m layers.....	37
Figure 22- Spatial distribution of HR70 $s_A$ at 70 kHz integrated in the first 100 m around ADR and FDN, averaged in grid size of 1 nm $\times$ 1 nm. Bottom depth contour lines in black for 100 (thick line), 300 and 500 m.....	37
Figure 23- Vertical distribution of HR70 $s_A$ values at 70 kHz greater than zero around ADR and FDN, averaged in layers each 10 m.....	38
Figure 24- Spatial distribution of fluid-like $s_A$ at 120 kHz integrated in the first 300 m around ADR and FDN, averaged in grid size of 1 nm $\times$ 1 nm. Bottom depth contour lines in black for 100 (thick line), 300 and 500 m.....	38
Figure 25- Vertical distribution of fluid-like $s_A$ values at 120 kHz greater than zero around ADR and FDN, averaged in layers each 10 m.....	39
Figure 26- Spatial distribution of HR38 <sub>1</sub> $s_A$ at 38 kHz integrated in the first 300 m around ADR and FDN, averaged in grid size of 1 nm $\times$ 1 nm. Bottom depth contour lines in black for 100 (thick line), 300 and 500 m.....	39
Figure 27- Vertical distribution of HR38 <sub>1</sub> $s_A$ values at 38 kHz greater than zero around ADR and FDN, averaged in layers each 10 m.....	40
Figure 28- Spatial distribution of HR38 <sub>2</sub> $s_A$ at 38kHz integrated in the first 300 m around ADR and FDN, averaged in grid size of 1 nm $\times$ 1 nm. Bottom depth contour lines in black for 100 (thick line), 300 and 500 m.....	40
Figure 29- Vertical distribution of HR38 <sub>2</sub> $s_A$ values at 38 kHz greater than zero around ADR and FDN, averaged in layers each 10 m.....	41
Figure 30- Spatial distribution of Unclassified $s_A$ at 70 kHz integrated in the first 300 m around ADR and FDN, averaged in grid size of 1 nm $\times$ 1 nm. Bottom depth contour lines in black for 100 (thick line), 300 and 500 m.....	41
Figure 31- Vertical distribution of Unclassified $s_A$ values at 70 kHz greater than zero around ADR and FDN, averaged in layers each 10 m.....	42

## Sumário

Página

Dedicatória

Agradecimentos

Resumo

Abstract

Lista de figuras

1- Introdução.....	11
1.1- Contextualização da pesquisa .....	11
1.2- Objetivo .....	13
2- Referências .....	13
3- Application of multifrequency acoustics to discriminate pelagic communities in oceanic islands of the tropical Atlantic off Brazil .....	16
4- Considerações finais .....	55
ANEXOS .....	56

## 1- Introdução

### 1.1- Contextualização da pesquisa

O arquipélago Fernando de Noronha (FDN, 03°51'S, 32°25' W) e o Atol das Rocas (ADR, 03°50' S, 33°49' W), que pertence à mesma cadeia de montes submarinos que FDN, estão inseridos em uma região oceânica de baixa produtividade e elevada biodiversidade (MILOSLAVICH et al., 2011). Esta área está influenciada pela Corrente Sul-Equatorial que transporta diferentes massas d'água em diferentes níveis de profundidade (STRAMMA and ENGLAND, 1999; PEREIRA et al., 2014).

ADR é o único atol do Atlântico Sul, e junto com FDN, são Unidades de Conservação no Brasil. A fauna de peixes nestas ilhas apresentam uma grande riqueza de espécies (117 e 169 respectivamente) e uma alta similaridade, compartilhando as mesmas 10 espécies endêmicas de peixes (SERAFINI et al., 2010). Muitas das espécies de peixes (*Caranx lugubris*, *Acantocybium solandri*, *Caranx latus*), crustáceos e moluscos que habitam nestas ilhas têm importância comercial (KIKUCHI, 1999), o que permite o desenvolvimento de uma importante pescaria artesanal em FDN (DOMINGUEZ, 2014). No entanto, fora da área de conservação das ilhas, existe uma importante atividade industrial, focada principalmente na pesca de espécies como a albacora laje (*Tunnus albacares*), o espadarte (*Xiphias gladius*) e o tubarão azul (*Prionace glauca*) (ZAGAGLIA et al., 2004; HAZIN et al., 2007). Adicionalmente, estas ilhas são uma considerável área de desova e alimentação para tartarugas e aves marinhas. Devido a sua importância, no ano 2001, estas ilhas foram declaradas patrimônio mundial pela UNESCO (UNESCO, 2016), e é necessária a aplicação de medidas de conservação.

As medidas de conservação requerem um enfoque ecossistêmico, o que em termos gerais significa reconhecer a interdependência entre o bem-estar humano e o do ecossistema (GARCIA et al., 2003). A implementação de um sistema de manejo baseado num enfoque ecossistêmico requer informações sobre as relações entre os componentes do ecossistema, e não apenas àqueles componentes de interesse comercial (TRENKEL e BERGER, 2013). Na atualidade, os sistemas de manejo incluem componentes espaciais, como as Áreas Marinhas Protegidas. A implementação destes sistemas requerem o estabelecimento de objetivos, protocolos e obtenção de informações em diferentes escalas, às vezes não disponíveis (ANDERSON et al., 2008).

Neste contexto, a única ferramenta que permite uma amostragem simultânea, em várias escalas espaço-temporal de informação qualitativa e quantitativa, desde o zooplâncton até os

VARGAS, G. O uso da acústica multifrequência na caracterização das comunidades pelágicas em ilhas oceâni...

predadores de topo, é a acústica submarina (BERTRAND et al., 2014), tornando-a uma ferramenta chave para a abordagem ecossistêmica. Considerando o espectro de luz visível para os humanos, só é possível ver poucos metros dentro d'água, este alcance se reduz no caso do meio apresentar sólidos em suspensão ou micro-organismos como o zooplâncton. No entanto, as ondas sonoras viajam distâncias maiores através d'água. O som (energia) é transmitido por compressões e expansões periódicas (ondas), o que é permitido pela elasticidade do meio. A energia é refletida por sólidos em suspensão, biota, borbulhas ou simplesmente convertida em calor por absorção física. Desta forma, os instrumentos acústicos que transmitem e recebem ondas sonoras podem ser usados para a detecção de uma variedade de componentes ecossistêmicos, do plâncton até os peixes, mas também estruturas físicas como gradientes térmicos, relevo submarino ou tipos de substrato (SIMMONDS and MACLENNAN, 2005; BERTRAND et al., 2014; BENOIT-BIRD and LAWSON, 2016).

Os dados acústicos coletados são representados em um ecograma. O ecograma é uma representação gráfica na qual a energia refletida pelos objetos na coluna d'água é plotado considerando o tempo e a profundidade (BENOIT-BIRD and LAWSON, 2016). No ecograma é possível classificar diferentes tipos de organismos. No entanto, para ter uma completa classificação é necessária alguma evidencia da composição biológica no meio através de coleta *in situ* (e.g. arrastos de pesca), ou também pode ser considerada a experiência do analista para identificar ecotipo (registros típicos) característico de cada espécie (SIMMONDS and MACLENNAN, 2005).

A intensidade da energia refletida pelos diferentes tipos de organismos é uma função do tamanho, forma, orientação e as propriedades dos materiais, assim como do comprimento de onda (STANTON and CHU, 2000). Porém, os organismos aquáticos geram diferentes respostas acústicas. Essa diferença é ainda maior quando se utilizam várias frequências. Sendo assim, é possível usar os padrões de dispersão para discriminar vários tipos de organismos distribuídos na coluna d'água (SIMMONDS and MACLENNAN, 2005).

Os conceitos sobre acústica multifrequência têm sido usados desde finais da década dos 70s, principalmente para quantificar populações de zooplâncton (GREENLAW, 1979; HOLLIDAY, 1980). Na atualidade é possível usar a acústica submarina e as propriedades físicas dos diferentes organismos para gerar ecogramas virtuais que permitem separar diferentes grupos de organismos na coluna d'água, segundo as suas diferenças de refletividade acústica (KORNELIUSSEN and ONA, 2002; DE ROBERTIS et al., 2010; BALLÓN et al., 2011; WOILLETZ et al., 2012; LEZAMA-OCHOA et al., 2014).

No Nordeste do Brasil a acústica submarina tem sido pouco usada. Uma prospeção acústica foi realizada dentro do programa REVIZEE, no ano 2004, usando a frequência de 38 kHz (WEIGERT and MADUREIRA, 2011). Isto significa que a prospeção acústica esteve orientada principalmente às comunidades de peixes e organismos grandes. As comunidades de zooplâncton não foram consideradas, uma vez que não é possível observar-lhes usando um limiar  $S_v$  de -60 dB. Para ter uma descrição detalhada das comunidades incluindo o zooplâncton e classifica outras comunidades é preciso a utilização da multifrequência.

## 1.2- Objetivo

Caracterizar e discriminar as comunidades pelágicas de peixes, zooplâncton, algas e outros ao redor do Arquipélago Fernando de Noronha e Atol das Rocas utilizando a acústica submarina. Também é objetivo deste trabalho o desenvolvimento de um módulo computacional para discriminar as comunidades pelágicas de peixes, zooplâncton, algas e outros ao redor do Arquipélago Fernando de Noronha e Atol das Rocas, que será usado para descrever a distribuição espaço temporal das diferentes comunidades pelágicas discriminadas.

## 2- Referências

- ANDERSON, J. T.; HOLLIDAY, D. V.; KLOSER, R. J.; REID, D. G.; SIMRAD, Y. Acoustic seabed classification: current practice and future directions. **ICES Journal of Marine Science**, v. 65, p. 1004–1011, 2008.
- BALLÓN, M.; BERTRAND, A.; LEBOURGES-DHAUSSY, A.; GUTIÉRREZ, M.; AYÓN, P.; GRADOS, D.; GERLOTTO, F. Is there enough zooplankton to feed forage fish populations off Peru? An acoustic (positive) answer. **Progress in Oceanography**, v. 91, p. 360–381, 2011.
- BENOIT-BIRD, K. J.; LAWSON, G. L. Ecological Insights from Pelagic Habitats Acquired Using Active Acoustic Techniques. **Review in Advance**, p. 1–28, 2016.
- BERTRAND, A.; GRADOS, D.; COLAS, F.; BERTRAND, S.; CAPET, X.; CHAIGNEAU, A.; VARGAS, G.; MOUSSEIGNE, A.; FABLET, R. Broad impacts of fine-scale dynamics on seascape structure from zooplankton to seabirds. **Nature Communications**, v. 5, 2014.
- DE ROBERTIS, A.; MCKELVEY, D. R.; RESSLER, P. H. Development and application of an empirical multifrequency method for backscatter classification. **Canadian Journal of Fisheries and Aquatic Sciences**, v. 67, p. 1459–1474, 2010.
- DOMINGUEZ, P. S. A pesca e o conhecimento local dos pescadores artesanais de Fernando

VARGAS, G. O uso da acústica multifrequência na caracterização das comunidades pelágicas em ilhas oceâni... de Noronha - PE. 2014. 69p. **Dissertação (Mestrado)** – Universidade Santa Cecília, São Paulo.

GARCIA, S. .; ZERBI, A.; ALIAUME, C.; DO CHI, T.; LASSERRE, G. **The ecosystem approach to fisheries**. Issues, terminology, principles, institutional foundations, implementation and outlook. FAO Fisheries Technical Paper. No. 443. Rome, FAO. 2003. 71p.

GREENLAW, C. Acoustical estimation of zooplankton populations. **Limnological Oceanography**, v. 24, p. 226–242, 1979.

HAZIN, H. G.; HAZIN, F.; TRAVASSOS, P.; CARVALHO, F. C.; ERZINI, K. FISHING STRATEGY AND TARGET SPECIES OF THE BRAZILIAN TUNA LONGLINE FISHERY , FROM 1978 TO 2005 , INFERRED FROM CLUSTER ANALYSIS. **Collective Volume of Scientific papers. ICCAT**, v. 60, p. 2029–2038, 2007.

HOLLIDAY, D. V. Volume scattering strengths and zooplankton distributions at acoustic frequencies between 0.5 and 3 MHz. **The Journal of the Acoustical Society of America**, v. 67, p. 135, 1980.

KIKUCHI, R. K. P. Atol das Rocas, Litoral do Nordeste do Brasil - Único atol do Atlântico Sul Equatorial Ocidental. **Sítios Geológicos e Paleontológicos do Brasil**, v. 1, p. 379–393, 1999.

KORNELIUSSEN, R. J.; ONA, E. An operational system for processing and visualizing multi-frequency acoustic data. **ICES Journal of Marine Science**, v. 59, p. 293–313, 2002.

LEZAMA-OCHOA, A.; IRIGOIEN, X.; CHAIGNEAU, A.; QUIROZ, Z.; LEBOURGES-DHAUSSY, A.; BERTRAND, A. Acoustics reveals the presence of a macrozooplankton biocline in the bay of Biscay in response to hydrological conditions and predator-prey relationships. **PLoS ONE**, v. 9, p. e88054, 2014.

MILOSLAVICH, P.; KLEIN, E.; DÍAZ, J. M.; HERNÁNDEZ, C. E.; BIGATTI, G.; CAMPOS, L.; ARTIGAS, F.; CASTILLO, J.; PENCHASZADEH, P. E.; NEILL, P. E.; CARRANZA, A.; RETANA, M. V.; DÍAZ DE ASTARLOA, J. M.; LEWIS, M.; YORIO, P.; PIRIZ, M. L.; RODRÍGUEZ, D.; VALENTIN, Y. Y.; GAMBOA, L.; MARTÍN, A. Marine biodiversity in the Atlantic and Pacific coasts of South America: Knowledge and gaps. **PLoS ONE**, v. 6, p. e14631, 2011.

PEREIRA, J.; GABIOUX, M.; MARTA-ALMEIDA, M.; CIRANO, M.; PAIVA, A. M.; AGUIAR, A. L. The bifurcation of the Western Boundary Current System of the South Atrantic Ocean. **Revista Brasileira de Geofísica**, v. 32, p. 241–257, 2014.



- VARGAS, G. O uso da acústica multifrequência na caracterização das comunidades pelágicas em ilhas oceânicas...
- SERAFINI, T. Z.; FRANÇA, G. B. De; ANDRIGUETTO-FILHO, J. M. Ilhas oceânicas brasileiras: biodiversidade conhecida e sua relação com o histórico de uso e ocupação humana. **Revista da Gestão Costeira Integrada**, v. 10, p. 281–301, 2010.
- SIMMONDS, J.; MACLENNAN, D. **Fisheries acoustics: theory and practice**. 2nd. ed., 2005. 325p.
- STANTON, T. K.; CHU, D. Review and recommendations for the modelling of acoustic scattering by fluid-like elongated zooplankton : euphausiids and copepods. **ICES Journal of Marine Science**, v. 57, p. 793–807, 2000.
- STRAMMA, L.; ENGLAND, M. On the water masses and mean circulation of the South Atlantic Ocean. **JOURNAL OF GEOPHYSICAL RESEARCH**, v. 104, p. 20863–20883, 1999.
- TRENKEL, V. M.; BERGER, L. A fisheries acoustic multi-frequency indicator to inform on large scale spatial patterns of aquatic pelagic ecosystems. **Ecological Indicators**, v. 30, p. 72–79, 2013.
- UNESCO. **World heritage papers 45. the future of the world heritage convention for marine conservation**, 2016. 147p.
- WEIGERT, S. C.; MADUREIRA, L. S. P. REGISTROS ACÚSTICOS BIOLÓGICOS DETECTADOS NA ZONA ECONÔMICA EXCLUSIVA DA REGIÃO NORDESTE DO BRASIL – UMA CLASSIFICAÇÃO EM ECOTIPOS FUNCIONAIS. **Atlântica**, v. 33, p. 15–32, 2011.
- WOILLEZ, M.; RESSLER, P. H.; WILSON, C. D.; HORNE, J. K. Multifrequency species classification of acoustic-trawl survey data using semi-supervised learning with class discovery. **The Journal of the Acoustical Society of America**, v. 131, p. 184–190, 2012.
- ZAGAGLIA, C. R. .; LORENZZETTI, J. A. .; STECH, J. L. Remote sensing data and longline catches of yellowfin tuna ( *Thunnus albacares* ) in the equatorial Atlantic. **Remote Sensing of /enviroment**, v. 93, p. 267–281, 2004.

### **3- Application of multifrequency acoustics to discriminate pelagic communities in oceanic islands of the tropical Atlantic off Brazil**

Gary Vargas

Universidade Federal Rural de Pernambuco (UFRPE), Departamento de Pesca e Aquicultura, Rua Dom Manoel de Medeiros s/n, Recife, Pernambuco, 52171-900, Brazil.

#### **Abstract**

Underwater acoustics have an unrealized potential for multicomponent ecosystem characterization. Various methods are used for multifrequency classification. To improve scatter discrimination we propose a new method based on the distribution of scatters on multifrequency spatial planes, to be applied in oceanic islands of the Northeast Brazil. Initially, groups of scatters are defined *a priori* from *in situ* sampling. Then we apply an objective separation criteria based in the maximum difference of cumulated energy to maximize energy allocation within a given group when compared to the nearest one. This method was applied on four frequencies (38, 70, 120 and 200 kHz) data collected in the frame of the ABRAÇOS (Acoustics along the BRAZilian COaSt) project, around Archipelago of Fernando de Noronha and Atoll das Rocas, an area characterized by low productivity but high biodiversity. By applying the method we discriminated six groups: Fish like, two types of High Resonant at 38 kHz associated to gelatinous, Fluid Like associated to crustacean macrozooplankton, High Resonant at 70 kHz associated to algae, and a group of Unclassified echoes. Results are coherent in terms of distribution pattern of each group. Among other, our results reveal that gelatinous are the dominant group close to oceanic islands where they form a dense layer above the thermocline. These results open new perspectives to improve knowledge on the patterns of distribution and the interaction of a variety of functional groups in different aquatic ecosystems.

**Keywords:** fish-like, fluid-like, algae echo, multifrequency algorithm, Fernando de Noronha

#### **Introduction**

The ecosystem approach to fisheries (EAF) is, in general terms, a strengthened approach that recognize the interdependence between human well-being and ecosystem well-being (GARCIA et al., 2003). The implementation of an EAF management requires a large amount of data, not only about the biomass of commercial species but also on the relationships between ecosystem components (TRENKEL et al., 2009). Nowadays, fisheries management also includes spatial components, such as Marine Protected Areas (MPAs) and fishery closed

areas. Implementing such management strategies requires the development of management objectives, protocols, and information at different spatial scales, not previously available (ANDERSON et al., 2008).

In this context, underwater active acoustics meets the features to be the only tool allowing the simultaneous collection, at a variety of spatiotemporal scales, of qualitative and quantitative data on the distribution and behavior, from plankton to large predators, including the habitat properties (BERTRAND et al., 2014). Indeed, at the wavelengths of human vision, light does not penetrate more than a few meters below the water surface. However, sound waves travel very much longer distances through water. Sound (energy) is transmitted by the periodic compression and expansion (waves). Energy is reflected (scattered) from the sound wave by suspended solids, biota or entrained gas. Therefore, the use of acoustic instruments (e.g. echosounders), which transmit and receive sound waves, can be used to detect fish or other objects far beyond the range of human vision (SIMMONDS and MACLENNAN, 2005).

The intensity of the backscattered energy is a complex function of organism size, shape, swimming orientation and anatomic physical properties, as well as acoustic frequency or wavelength (STANTON and CHU, 2000). According to their physical characteristics (shape, presence of swimbladder, etc.) organisms exhibit specific frequency responses of great value for remote inference of community composition using multifrequency methods. Multifrequency techniques take advantages of the characteristics of the organisms, making possible an automatic classification of the different categories of organisms (DE ROBERTIS et al., 2010; BALLÓN et al., 2011; TRENKEL and BERGER, 2013; LEZAMA-OCHOA et al., 2014; BENOIT-BIRD and LAWSON, 2016; KORNELIUSSEN et al., 2016).

The acoustic properties of a variety of types of scatters have been documented. Swimbladder-bearing fish have high and homogenous backscattering response at each frequency (FOOTE, 1985; COCHRANE et al., 1991; KORNELIUSSEN and ONA, 2002). Crustaceans (e.g. euphausiids, copepods) have a body with acoustic properties similar to those of the medium and are classified as 'fluid-like'. They are characterized by a backscattering response higher at high than at low frequencies (GREENLAW, 1979; HOLLIDAY, 1980; DEMER and CONTI, 2005; BENOIT-BIRD and LAWSON, 2016). Many gelatinous have a soft body together with a gas bubble inclusion (gas-bearing), providing a strong backscattering at low frequencies, in particular at 38 kHz. Gas-bearing gelatinous are thus highly resonant at 38 kHz (STANTON et al., 1998; BRIERLEY et al., 2001, 2004; TREVORROW et al., 2005). Other organisms can share such characteristics, in particular fish

larvae (WOILLEZ et al., 2012; BENOIT-BIRD and LAWSON, 2016). Finally, a recent study (LEBOURGUES-DHAUSSY et al., 2016) showed that algae have a higher acoustic response at 70 kHz.

Substantial progress has been made in multifrequency echo-classification in recent years. However, the utility and effectiveness of any particular approach depend on the characteristics of the communities present in the ecosystem where they are applied. Indeed, classification success depends on the species composition, relative abundance, relative frequency response, and spatial overlap of the species assemblage present in the environment (DE ROBERTIS et al., 2010). Therefore, the complexity of the application of multifrequency acoustic methods increases when performed in highly diverse tropical systems.

Around the Archipelago of Fernando de Noronha (FDN, 03°51'S, 32°25' W) and Atoll das Rocas (ADR, 03°50' S, 33°49' W), active underwater acoustic has not been widely used (WEIGERT and MADUREIRA, 2011). These oceanic islands are located in Northeast Brazil, a region of low productivity but high biodiversity (MILOSLAVICH et al., 2011), influenced by the South Equatorial Current (SEC) (STRAMMA and ENGLAND, 1999; RODRIGUES et al., 2007; PEREIRA et al., 2014). ADR is the unique south Atlantic atoll, and was the first Marine Protected Area (MPA) created in Brazil. In FDN and ADR there is a large amount of commercial fish (*Caranx lugubris*, *Acantocybium solandri*, *Caranx latus*), molluscs and crustaceans species (KIKUCHI, 1999), that allow the developing of an important artisanal fishery (DOMINGUEZ, 2014). However, out of MPA exists an industrial activity focused in the fishery of species as yellowfin tuna (*Tunnus albacares*), swordfish (*Xiphias gladius*) and blue shark (*Prionace glauca*) Due to the distance from the continent, these systems have a particular biodiversity and still harbor a large number of endemic species (SERAFINI et al., 2010). Because of their importance, these oceanic islands have been included into the UNESCO World Heritage List in 2001 (UNESCO, 2016).

In this study the multifrequency acoustics data and biological samples collected around ADR and FDN were used to develop a methodology to discriminate between different pelagic communities (i.e. fish, zooplankton, gelatinous and algae). The application of the methods allowed identifying and quantifying the acoustic biomass of each group, and to study the ecosystem in 3D.

## **Material and Methods**

### **Acoustic data collection**

Data were collected during the acoustic “ABRAÇOS” survey performed around the Archipelago of Fernando de Noronha, the “Atoll das Rocas”, and along the coast from Natal to North of Alagoas in Northeast Brazil, aboard the R/V “Antea” (35 m long), between September 29<sup>th</sup> - October 21<sup>st</sup>, 2015 (Fig. 1). The survey track consisted in daisy-pattern transects around the islands and in cross-shore transects between 15 to 30 nm along the coast with a mean vessel speed of 8.5 knots. Acoustic data were collected continuously (from 0 to 750 m depth) during transects but also at each stations, using a Simrad EK60 (Kongsberg Simrad AS) split-beam scientific echosounder at 38, 70, 120 and 200 kHz. The echosounder was previously calibrated (FOOTE et al., 1987) using a tungsten carbide sphere. Here mostly the acoustic data corresponding to the oceanic islands of the Archipelago of Fernando de Noronha (FDN) and of Atoll das Rocas (ADR) were used (Fig. 1).

In acoustic data, the energy of each echo is expressed in terms of ‘area’, that is, organisms from the same specie with different size will reflect an area value proportional to their size. This area is known as backscattering cross-section area ( $\sigma_{bs}$  in  $m^2$ ), but is more commonly used its logarithmic expression, called Target Strength (TS in dB re 1  $m^2$ ). However, due to the propagation, the volume covered by the acoustic axis increases according to depth. Therefore, to quantify the biomass it is better to use a unity corresponding to a density. This unity is known as volume backscattering coefficient ( $S_v$  in dB re 1  $m^2 m^{-3}$ ), and is the logarithmic expression of the  $\sigma_{bs}$  accumulated into a water volume of 1  $m^3$  (MACLENNAN et al., 2002; SIMMONDS and MACLENNAN, 2005).

### **Biological sampling**

*In situ* sampling for acoustic echo identification was performed using mesopelagic trawl (n=31) with 4 mm cod-end mesh, and equipped with a Time Depth Recording (TDR) system. Additionally, zooplankton was sampled using bongo oblique trawls (n=33, mesh sizes: 500, 300, 120 and 64  $\mu m$ ), from 200 m or 10 m over the seabed to the surface. Samples were frozen (trawl) or fixed in formaldehyde (zooplankton) before identification and quantification at the laboratory.

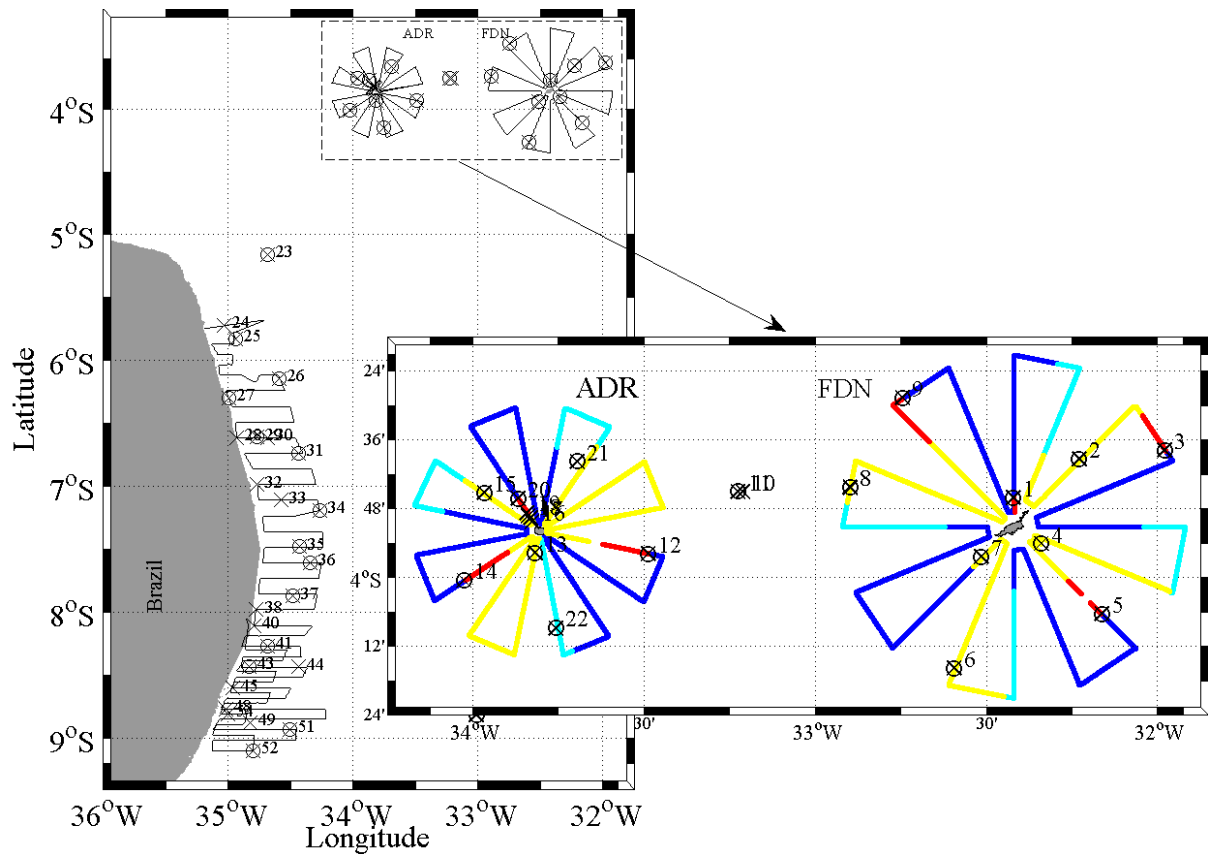


Figure 1- ABRAÇOS survey track and sampling around the Archipelago of Fernando de Noronha (FDN) and Atoll das Rocas (ADR). The colors depicts the diel cycle: day in yellow, dusk in red, night in blue and dawn in cyan. Bongo stations are represented by black circles and mesopelagic trawls by black crosses.

### Acoustics data analysis

The different steps of the multifrequency algorithm developed in Matlab (MathWorks™, Natick, Massachusetts, USA) are synthetized in Figure 2. A small part of the code is presented in Annex 1. The criteria to determine thresholds used in this method will be detailed below.

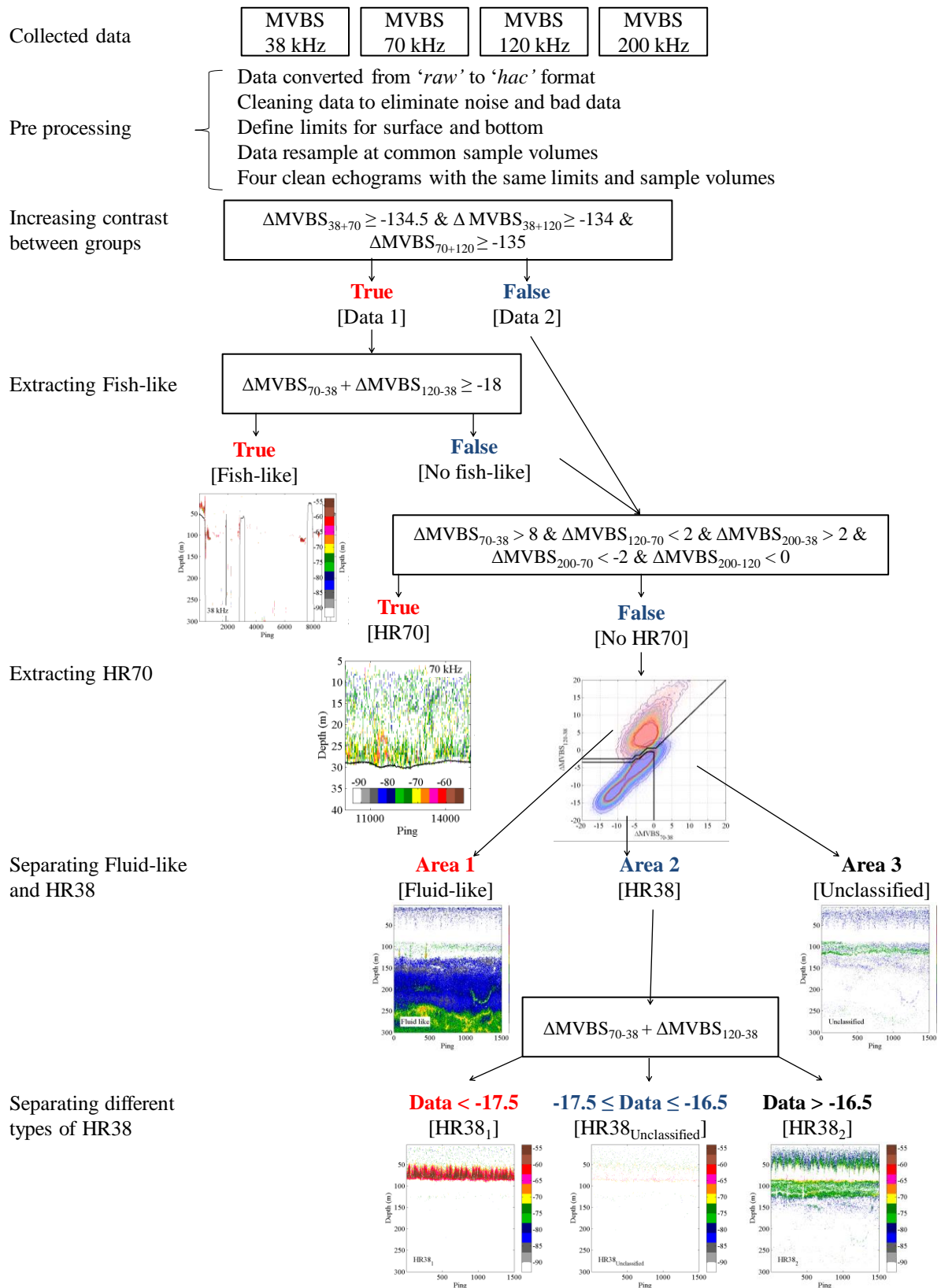


Figure 2- Flow chart of the multifrequency method for scatter discrimination

### **Pre-processing**

The digital files of acoustic data were converted from 'raw' to 'hac' files using ER60 (Kongsberg Simrad AS) and Hermes (TRENKEL et al., 2009) software. Automatic algorithms developed in Matlab (MathWorks™, Natick, Massachusetts, USA) were used to extract the background noise (DE ROBERTIS and HIGGINBOTTOM, 2007) as well as the other noise types (RYAN et al., 2015). To correct the bottom line and verify that all noises, interferences, and erroneous data were excluded, a visual scrutinizing was carried out using Movies 3D software (TRENKEL et al., 2009).

To reduce high frequency variability, the acoustic data (expressed in  $S_v$ ) were averaged by bins of 0.5 m thick (DE ROBERTIS et al., 2010; BALLÓN et al., 2011; WOILLEZ et al., 2012). The averaged expression of  $S_v$  is named mean volume backscattering coefficient (MVBS, in dB re  $1 \text{ m}^2 \text{ m}^{-3}$ ). The first 5 m from the surface were excluded to eliminate the near field and the influence of absorption and propagation. Acoustic data at 38, 70 and 120 kHz were processed up to 300 m (or to the bottom if less than 300 m), while 200 kHz were processed up to 150 m (or to the bottom if less than 150 m). The result was a clean matrix (for each frequency) of mean volume backscattering strength (MVBS, in dB re  $1 \text{ m}^2 \text{ m}^{-3}$ ) in two dimensions: vertical samples each 0.5 m and horizontal samples each ping (about 1 s). To reduce the variability and improve the discrimination between the classes of echoes, a convolution was applied to echograms, i.e., the value of each individual cell was averaged with their immediate eight neighbors.

### **Separating fish-like echoes**

Four steps were employed to discriminate the echoes attributed to fish. First, several sections of echograms containing echotraces with characteristics alike to fish schools were selected. Second, a threshold at 38 kHz was applied to exclude weak echoes unlikely corresponding to fish. This threshold was set up at -69 dB, because the selected data presented a distribution with two modes (Annex 2), one in -85 dB (very low to be fish) and -59 dB (compatible with fish). Among the selected echotraces ( $MVBS_{38} \geq -69 \text{ dB}$ ), two groups with different multifrequency responses were identified (Fig. 3). A group presented homogenous MVBS values (around -60 dB) at all frequencies, as expected for swimbladder-bearing fish (BENOIT-BIRD and LAWSON, 2016), while the other group (no fish) presented higher values at 38 than 70 and 120 kHz (Fig. 4).



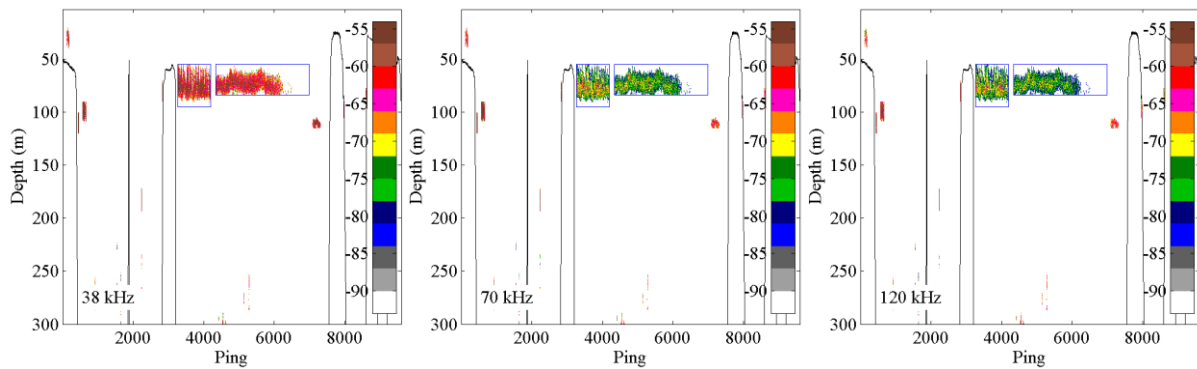


Figure 3- Echotrases selected ( $MVBS_{38} \geq -69$  dB). Blue boxes highlight echotrases with acoustic response higher at 38 kHz than at 70 and 120 kHz (unlikely fish-echoes), the other echotrases present high and homogeneous acoustic response (typical for fish). The black line represents the seafloor.

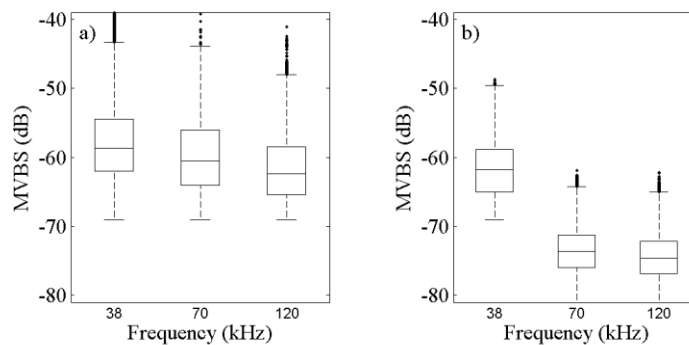


Figure 4- MVBS multifrequency response of the two groups of selected data ( $MVBS_{38} \geq -69$  dB): a) fish-like echoes and b) no fish-like echoes.

Third, to define objective criteria to separate between the two groups, the sum of the frequencies ( $+MVBS_{70+120}$ ,  $+MVBS_{38+70}$  and  $+MVBS_{38+120}$ ) was used. This approach allows enhancing the contrast between swimbladder-bearing fish that have strong echoes at all frequencies and other organisms, making them easier to discriminate (BALLÓN et al., 2011; LEZAMA-OCHOA et al., 2014). Indeed, according to Figure 4, fish-like echoes were expected to have  $+MVBS_{70+120}$  significantly higher than no fish-like echoes. To determine the best thresholds to discriminate between groups, objective separation criteria based in the maximum difference of cumulated energy were used. Explicitly, the percentage of energy of echoes with fish-like and no fish-like characteristics cumulated along  $+MVBS_{70+120}$  were determined, then the threshold maximizing the difference among groups was determined. Results (Fig. 5) show that the best threshold for  $+MVBS_{70+120}$  was  $-135$  dB (no fish-like  $< -135 \leq$  fish-like). For  $+MVBS_{38+70}$  and  $+MVBS_{38+120}$  the difference between groups was too

weak to determine a threshold in the same way. For this reason, the threshold was set where 99.5% of the energy of the fish-like group was accumulated, i.e., at -134.5 and -134 dB for +MVBS<sub>38+70</sub> and +MVBS<sub>38+120</sub>, respectively.

Fourth, the group with data above the threshold for each sum of frequencies (fish-like echoes candidate) was considered for further analyses. The difference between frequencies ( $\Delta$ MVBS) was used to eliminate echoes classified in this group but containing echoes from scatters not originated by fish. This method is commonly used to discriminate between acoustics groups (Murase et al. 2009; Ballón et al. 2011; Trenkel & Berger 2013; Lezama-Ochoa et al. 2014). The echoes were plotted according to all possible frequency differences. In Figure 6a the X-axis corresponds to the difference between 70 and 38 kHz ( $\Delta$ MVBS<sub>70-38</sub>), the Y-axis corresponds to  $\Delta$ MVBS<sub>120-38</sub>, finally the diagonal axis (1,0  $\rightarrow$  0,1) mathematically defined as  $\Delta$ MVBS<sub>120-38</sub> -  $\Delta$ MVBS<sub>70-38</sub>, corresponds to  $\Delta$ MVBS<sub>120-70</sub>. To discriminate between fish-like echoes (low difference between frequencies) and the residual no fish-like echoes (higher response at 38 kHz) the more discriminant axis was the other diagonal axis (0,0  $\rightarrow$  1,1), mathematically defined as  $\Delta$ MVBS<sub>70-38</sub> +  $\Delta$ MVBS<sub>120-38</sub>. On this axis, the objective separation criteria allowed to set up the threshold at -18 dB (Fig. 6b). Finally, a convolution was applied to recover all voxels that could have been left out in the fish-like group. It allows including the nearest neighbor voxels that could contain fishes-like echoes (Fig. 7).

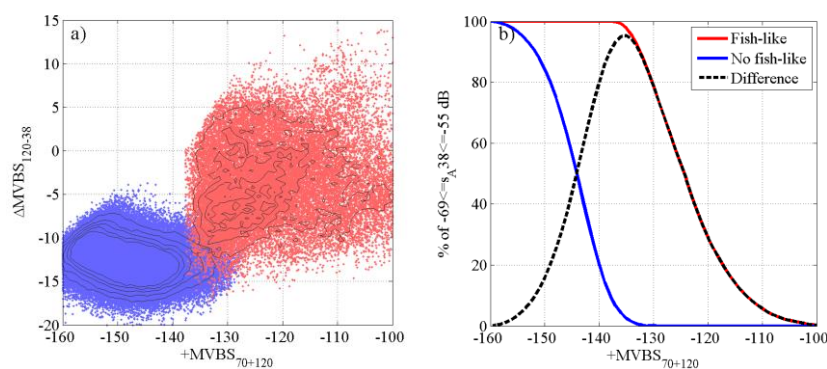


Figure 5- a) Data distribution of fish-like echoes (red points) and no fish-like echoes (blue points), the contour lines represents spatial density of the data. b) Objective separation criteria: % of energy of fish-like (red line) and no fish-like (blue line) echoes cumulated from -100 dB to -160 dB along +MVBS<sub>70+120</sub>. The black line shows the difference among groups; the corresponding value at X axis (-135 dB) with maximum difference defines the best limit to discriminate between the two groups.

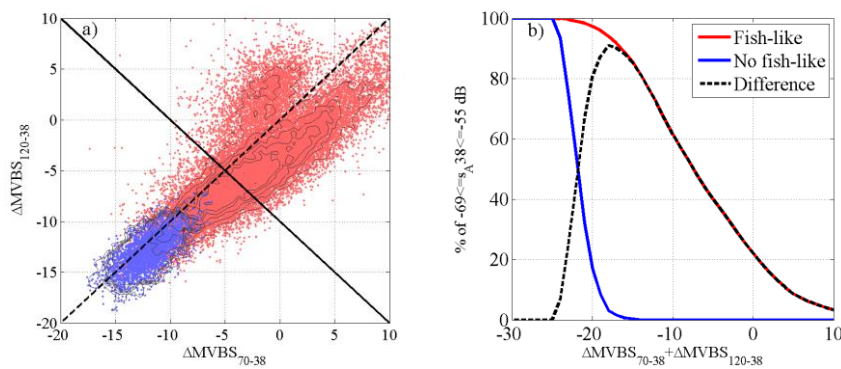


Figure 6- a) Data distribution of fish-like echoes (red points) and no fish-like echoes (blue points), the contour lines represents spatial density of the data. b) Objective separation criteria: % of energy of fish-like (red line) and no fish-like (blue line) echoes cumulated from -25 to 10 dB along  $\Delta MVBS_{70+38} + \Delta MVBS_{120+38}$ . The black line shows the difference among groups; the corresponding values at X axis (-18 dB) with maximum difference defines the best limit to discriminate between the two groups.

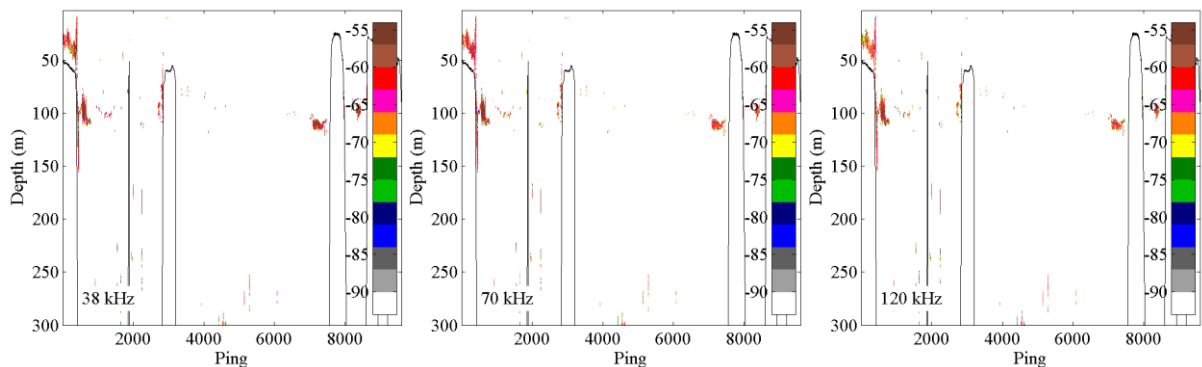


Figure 7- Final fish-like echograms at 38, 70 and 120 kHz. The black line represents the seafloor.

### Separating High Resonant at 70 kHz echoes

During the survey, high resonant echoes at 70 kHz (HR70), that is, the echoes with highest response at 70 kHz, were associated to pelagic algae (LEBOURGÉS-DHAUSSY et al., 2016). To setup the algorithm to discriminate HR70 the station 33 (7°07' S, 34°35' W) was used, because there was visual confirmation of the dominance of pelagic algae (Fig. 8). The process, applied on no fish-like data, is based on the multifrequency response distribution of this group ( $MVBS_{70} > MVBS_{120} > MVBS_{200} > MVBS_{38}$ ) and was divided into four steps.

First, only the first 5 m from the bottom were used because this layer presented positive and homogeneous  $\Delta MVBS_{70-38}$  values (mean  $> \sim 8$  dB). To eliminate extreme values of the

distribution, echoes where  $\Delta MVBS_{70-38} \leq 0$ ,  $\Delta MVBS_{120-38} \leq 0$ ,  $MVBS_{70} \leq -80$  dB and  $MVBS_{200} \geq -73$  dB were excluded.

Second, to refine the selection and exclude the final part of the tail of distribution (0.5% of the data) along the X-axis of frequency differences ( $\Delta MVBS_{120-70}$ ,  $\Delta MVBS_{200-70}$ ,  $\Delta MVBS_{200-120}$ ), the echoes distributed off the threshold, corresponding to more than 99.5% of the cumulated energy were eliminated. The corresponding thresholds were 2, -2 and 0 dB for  $\Delta MVBS_{120-70}$ ,  $\Delta MVBS_{200-70}$  and  $\Delta MVBS_{200-120}$ , respectively.

Third, the previous settings were applied to an echogram for which the absence of pelagic algae was confirmed (Station 6, 4°15'S, 34°37'W, layer depth: 100 - 150 m). Part of the echoes was not eliminated. Thus, improve the settings was necessary. For that purpose, the distribution of the resultant echoes from Stations 6 and 33 were compared along the axis  $\Delta MVBS_{70-38}$ . Applying an objective separation criteria (Fig. 9a), the threshold was defined at 8 dB (no  $HR_{70} \leq 8 < HR_{70}$ ).

Fourth, a new objective separation criteria was set up along  $\Delta MVBS_{200-38}$  on the data selected in the previous step. The threshold was defined at 2 dB (Fig. 9b). In synthesis, the thresholds to discriminate  $HR_{70}$  scatters were:  $\Delta MVBS_{120-70} < 2$ ,  $\Delta MVBS_{200-70} < -2$ ,  $\Delta MVBS_{200-120} < 0$ ,  $\Delta MVBS_{70-38} > 8$  and  $\Delta MVBS_{200-38} > 2$ . The Figure 10 shows the echogram obtained at the end of this process.

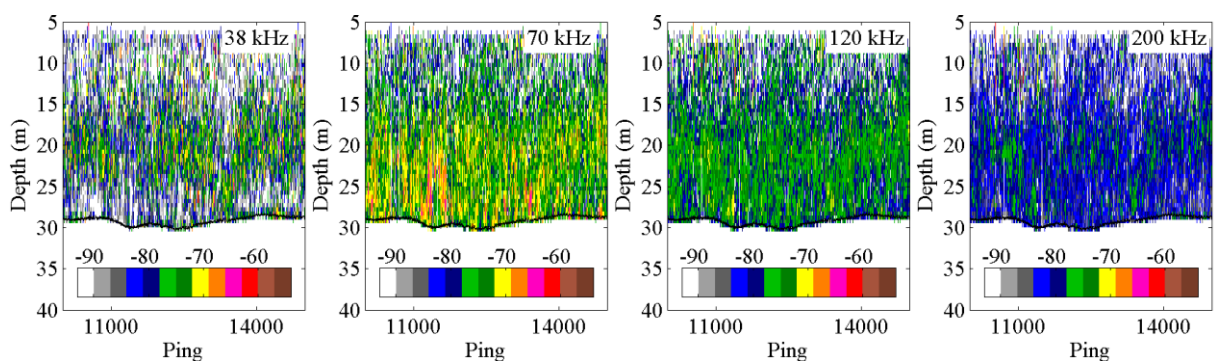


Figure 8- Echograms from Station 33, where the presence of algae was confirmed visually.

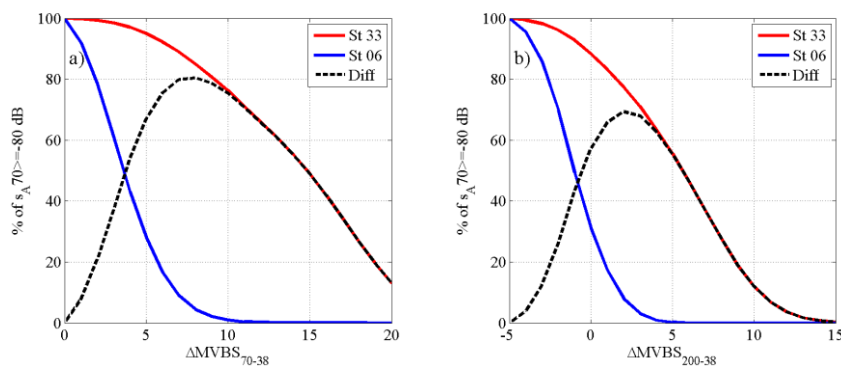


Figure 9- Objective separation criteria: % of energy cumulated from data selected of Station 33 (HR70) in red line and data selected of Station 06 (no HR70) in blue line from 0 to 20 dB along a)  $\Delta MVBS_{70-38}$  and from -5 to 15 dB along b)  $\Delta MVBS_{200-38}$ . The black line shows the difference among groups; the corresponding values at X axis (8 dB for  $\Delta MVBS_{70-38}$  and 2 dB for  $\Delta MVBS_{200-38}$ ) with maximum difference defines the best limit to discriminate between the two groups.

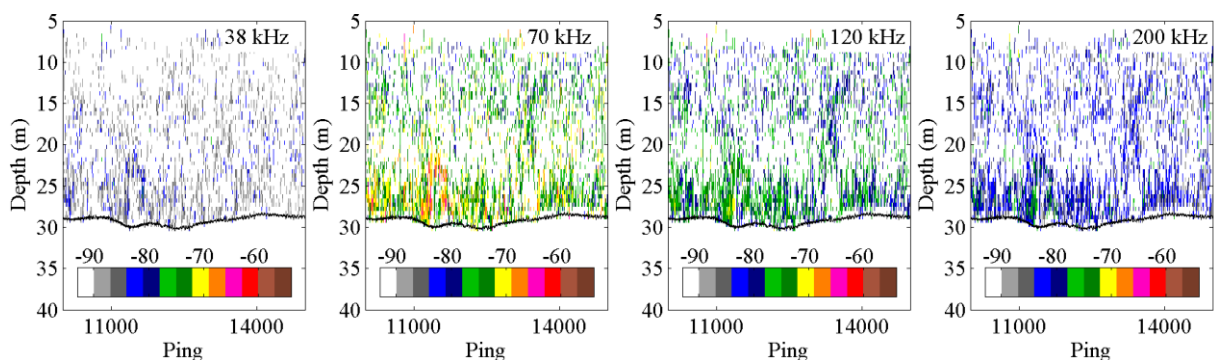


Figure 10- Final HR70 echograms at 38, 70, 120 and 200 kHz.

### Separating Fluid-like, High Resonant at 38 kHz and Unclassified echoes.

At this stage, the resultant data (no fish-like and no HR70) presented diverse characteristics. Part of the echoes presented the characteristics of fluid-like scatters (Fig. 11a): highest MVBS at high frequency (120 or 200 kHz). The other scatters (Fig. 11b) had highest response at 38 kHz and were classified as high resonant at 38 kHz (HR38). To discriminate between these scatters, the data were plotted according to all possible frequency differences. In Figure 11c the X-axis corresponds to  $\Delta MVBS_{70-38}$ , the Y-axis to  $\Delta MVBS_{120-38}$  and the diagonal axis (1,0  $\rightarrow$  0,1) to  $\Delta MVBS_{120-70}$ . In this space, the limit maximizing the difference between the groups of scatters was determined in the multidimensional space [ $\Delta MVBS_{70-38}$ ;  $\Delta MVBS_{120-38}$ ], the resulting threshold being a line, not a point (Annex 3). Still, some echoes

of each group exceeded the limit. To reduce misclassification added new constraints were added. For each axis the limit corresponding to the 99.5% of cumulated energy of each group was determined. These thresholds were -3, 0 and 0 dB for  $\Delta MVBS_{70-38}$ ,  $\Delta MVBS_{120-38}$  and  $\Delta MVBS_{120-70}$ , respectively (Fig. 11c). This step allowed discriminating between fluid-like and HR38 echoes, and led us to define a new group that could not be classified that was named Unclassified. Finally, to ensure the robustness of the classification and prevent possible overlap between groups a 1 dB thick band was added between fluid-like and HR38. The corresponding echoes were added to the Unclassified group. The Figure 11d,e,f shows the echogram obtained at the end of this process.

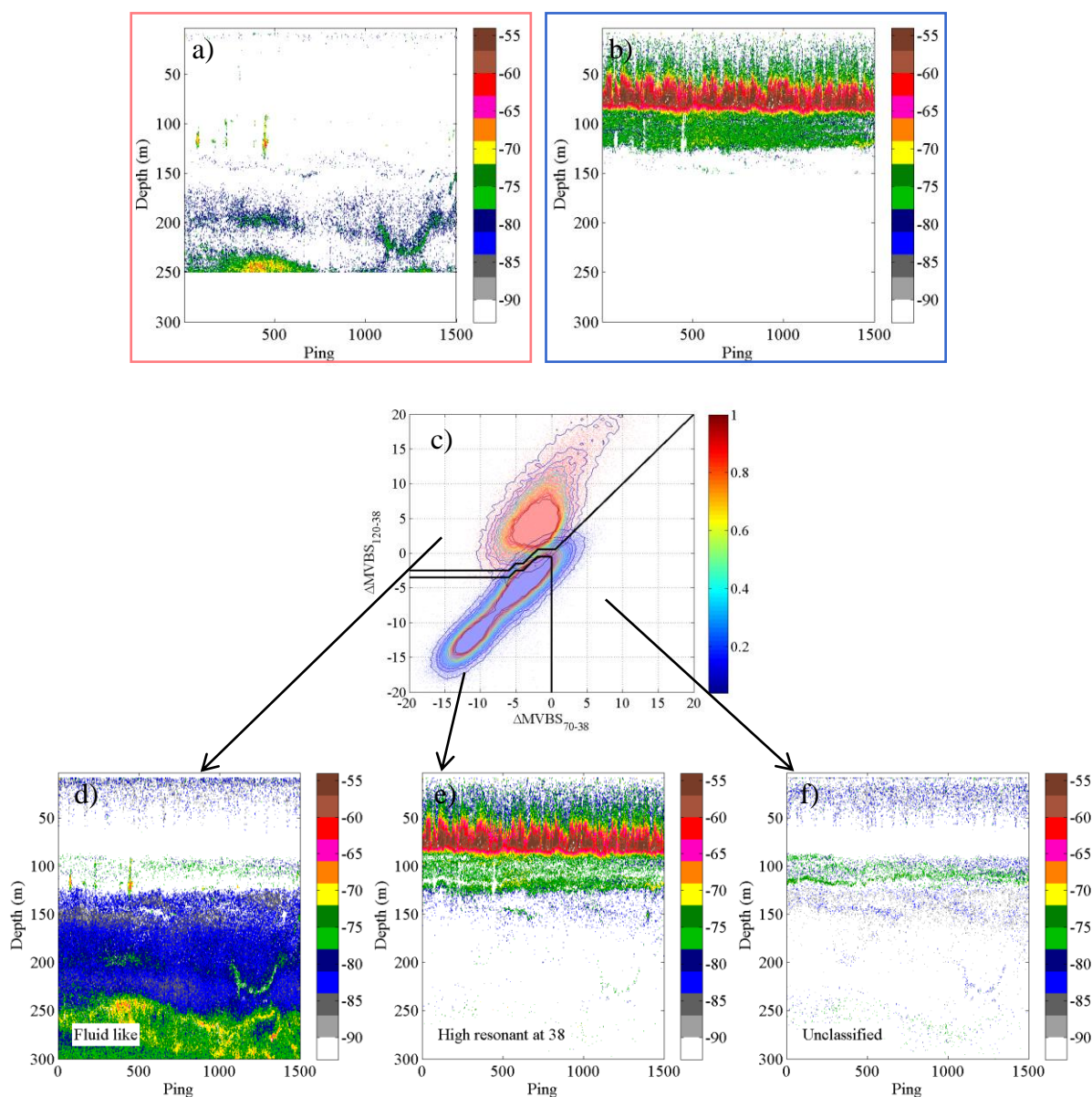


Figure 11- Process to discriminate Fluid like, HR38 and Unclassified. Two groups, one with a) highest MVBS at 120 or 200 kHz, another with b) highest MVBS at 38 kHz were selected

and c) plotted, the contour lines represents spatial density of the data. The multidimensional objective separation criteria divided the plane in 3 regions: d) Fluid-like, e) HR38 and f) Unclassified echoes.

### **Separating HR38<sub>1</sub> and HR38<sub>2</sub> echoes**

The HR38 was not homogeneous and presented diverse characteristics. To compare these differences, two layers were selected; one between 60 and 85 m and the other from 95 to 130 m (Fig. 12a). The data between 85 and 95 m was not used to avoid overlapping data between groups. The first layer was more resonant at 38 kHz than the deeper one. To separate these groups an objective separation criteria was set up using the more discriminant axis, mathematically defined as  $\Delta MVBS_{70-38} + \Delta MVBS_{120-38}$  (Fig. 12b). On this axis, the objective separation criteria allowed to set up the threshold at -17 dB. Additionally, to ensure the robustness of the classification and prevent possible overlap between groups, a 1 dB thick band was added between HR38<sub>1</sub> and HR38<sub>2</sub>. The corresponding echoes were named HR38<sub>Unclassified</sub>. In synthesis, the thresholds were defined as:  $HR38_1 < -17.5 \text{ dB} \leq HR38_{\text{Unclassified}} \geq 16.5 > HR38_2$ . The Figure 12c,d,e shows the echogram obtained at the end of this process.

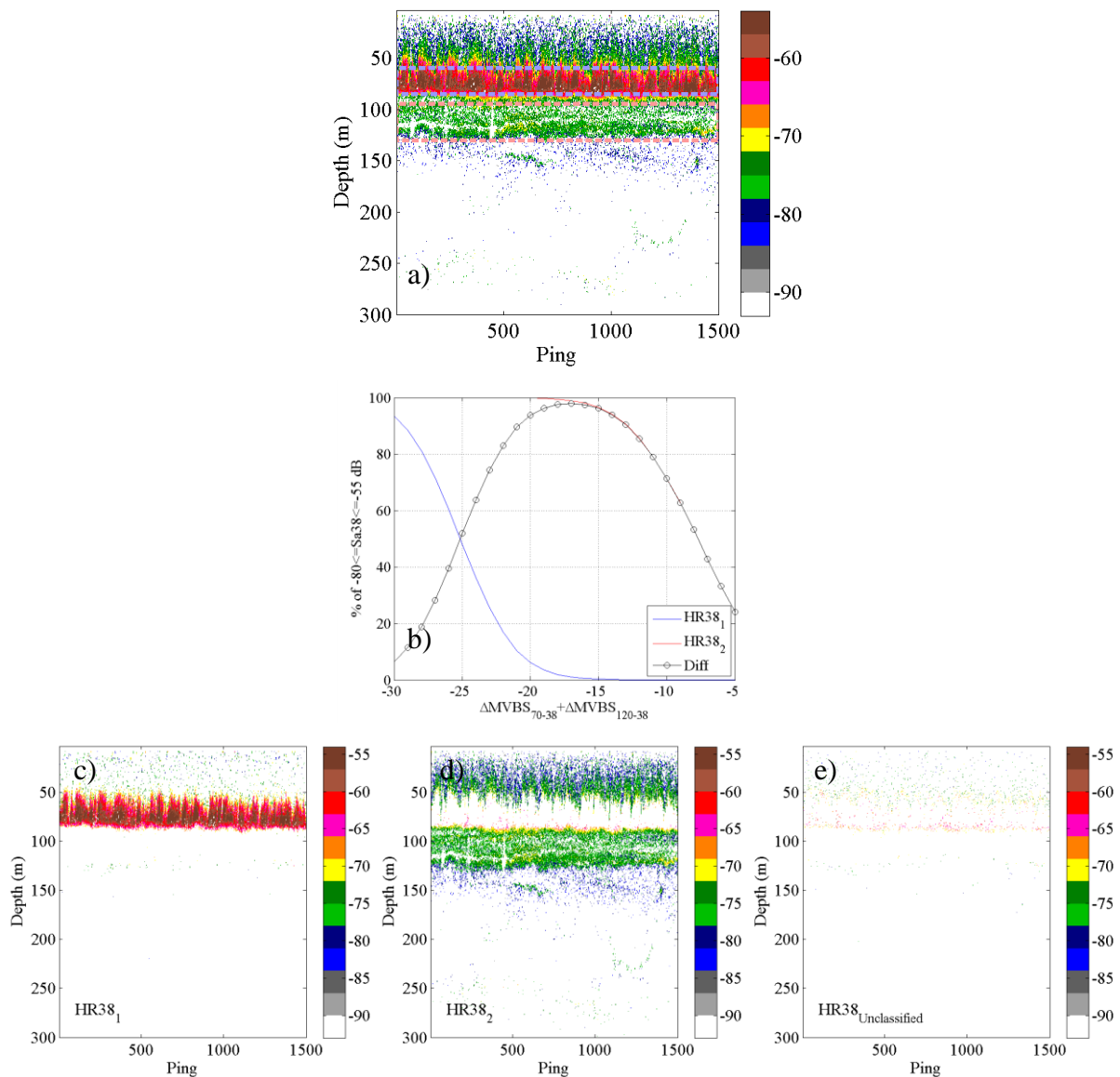


Figure 12- Process to separate HR38 echoes. Two layers, a) the first with MVBS echoes more resonant (named HR38<sub>1</sub> in blue dashed line box) than the b) second (named HR38<sub>2</sub> in red dashed line box) at 38 kHz were extracted and a c) Objective separation criteria was performed: % of energy of HR38<sub>2</sub> (red line) and HR38<sub>1</sub> (blue line) echoes cumulated from -30 dB to -5 dB along  $\Delta MVBS_{70-38} + \Delta MVBS_{120-38}$ . The black line shows the difference among groups; the corresponding value at X axis (-17 dB) with maximum difference defines the best limit to discriminate between the two groups. Additionally, a band 1 dB thick was added between HR38<sub>1</sub> and HR38<sub>2</sub> to prevent possible overlap between them, for this reason the HR38 scatters was separated in 3 groups: d) HR38<sub>1</sub>, e) HR38<sub>2</sub> and f) the group named H38<sub>Unclassified</sub>.



## Validation

To determine if the identified acoustic groups actually correspond to biological communities a validation process is required. For that purpose the acoustic energy of the different groups was compared with the trawl catches.

**Fish-like, and HR38:** The data from Time Depth Recorder (TDR) installed on the trawl net, allowed to precisely delineate the echogram section sampled by the trawl (Fig. 13). The acoustic energy into trawl echogram section ( $S_{A\ trawl}$ ) was extracted from fish-like (only night samples) and HR38. The catch was classified and weighed in two groups: total fish to compare with fish-like echoes and gelatinous with larvae fish to compare with HR38. In order to relate the  $S_{A\ trawl}$  values of each group with trawl catches (in g), the  $S_{A\ trawl}$  was multiplied by the trawled distance ( $dist_{trawl}$  in nm). The data was normalized using  $\text{Log}_{10}(x+1)$ . To quantify the relationship between  $[S_{A\ trawl} \times dist_{trawl}]$  and trawl catch a Pearson correlation analysis was performed.

**HR70:** During the survey, the *in situ* sampling of pelagic algae was not optimal. For this reason the validation of the HR70 group was performed using as reference the  $S_A$  of HR70 scatters with  $MVBS70 > -90$  dB in Stations 18, 33, (where there had visual confirmation of algae presence) and 55 (where there had not visual algae presence).

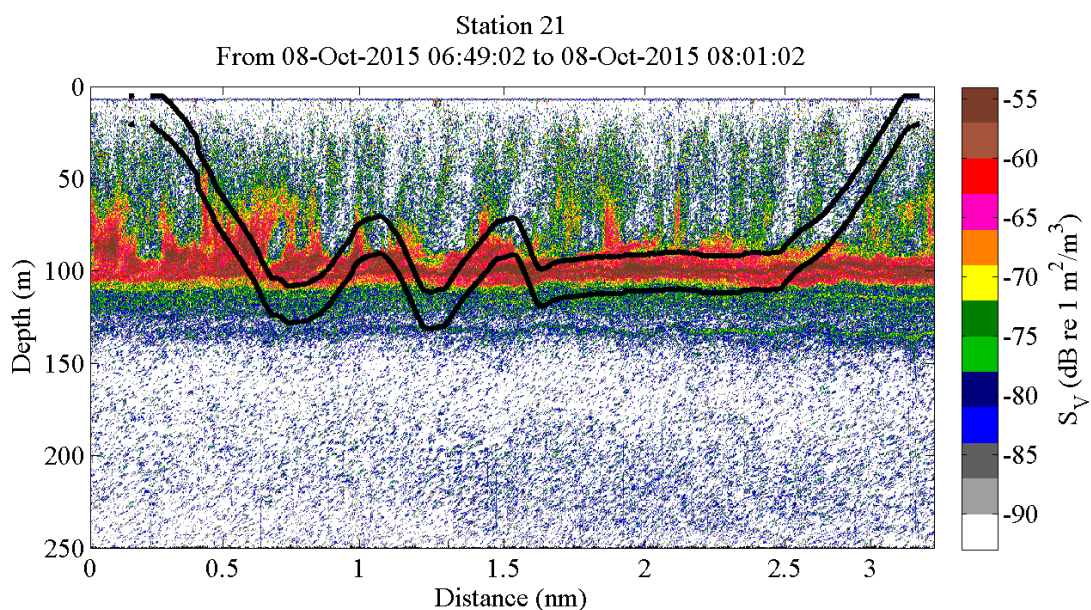


Figure 13- Example of synchronization between acoustic and TDR data (Station 21). The black line represents the path followed by the fishing gear during the trawl.

### **Estimation of acoustic biomass**

To obtain an estimate of the acoustic biomass for each group, the corresponding MVBS was integrated from the bottom (or 300 m) to the surface. This acoustic biomass is defined as acoustic nautical area scattering coefficient ( $s_A$  in  $m^2 \text{ nm}^{-2}$ ) and calculated using:

$$s_A = 4\pi (1852)^2 \int_{z_1}^{z_2} S_V dz \quad \text{Eq. (1)}$$

where  $S_V$  corresponds to the MVBS, and  $z_1$  and  $z_2$  are the surface and bottom depth, respectively (MACLENNAN et al., 2002).

The  $s_A$ , which is an indicator of the biomass (SIMMONDS and MACLENNAN, 2005), was averaged in a grid with a resolution of 1 nm, to observe the spatial distribution of each group.

To seek for potential diel effect on the biomass of each group in the studied water column, a Student t-test was used to test for significant differences between day and night periods.

## **Results**

### **Validation**

The Pearson correlation analysis performed to validate acoustic biomass of fish-like and HR38 with the trawl catches (Fig 14) showed that there is positive and significant correlation for the both of them. However Fish-like ( $r = 0.8160$ ,  $n = 10$ ,  $p = 0.0031$ ) presented a higher correlation than and HR38 ( $r = 0.4861$ ,  $n = 18$ ,  $p = 0.0397$ ).

No quantitative validation could be achieved for HR70 since pelagic algae have not been sampled in a quantitative way. The application of the algorithm in stations 18 and 33 where pelagic algae have been observed (ABRAÇOS, unpublished data) led to an acoustic biomass of HR70 of 8.2 and 9.7  $m^2 \text{ nm}^{-2}$ , respectively. These acoustic biomass, despite to be numerically small, are higher when compared with the common HR70 biomass values found during the survey (see Figs. 19 and 22). Conversely, when applying the algorithm in Station 55 (where no pelagic algae were observed), the biomass of HR70 group for scatters with  $MVBS_{70} > -90$  dB was calculated in 0.6  $m^2 \text{ nm}^{-2}$ .

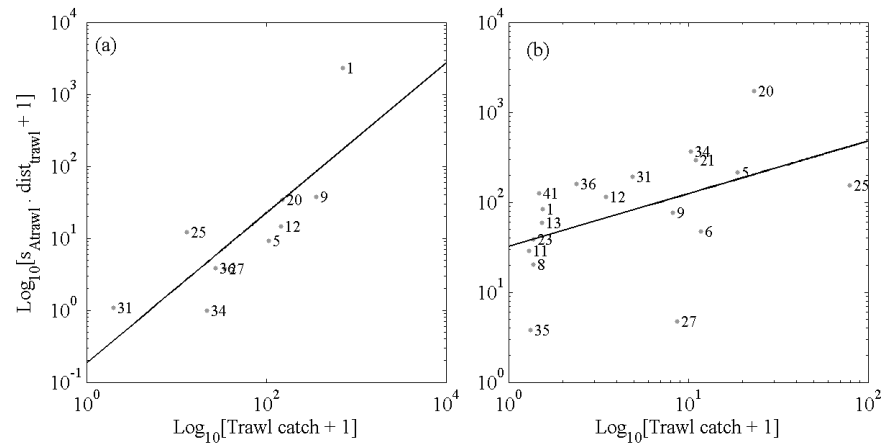


Figure 14- Scatter plot of acoustic energy in the trawled area (in  $\log_{10} [s_{A\text{trawl}} \cdot \text{dist}_{\text{trawl}} + 1]$ ) versus trawl catch (in  $\log_{10}[\text{Trawl catch} + 1]$ ), for (a) fish-like and (b) HR38.

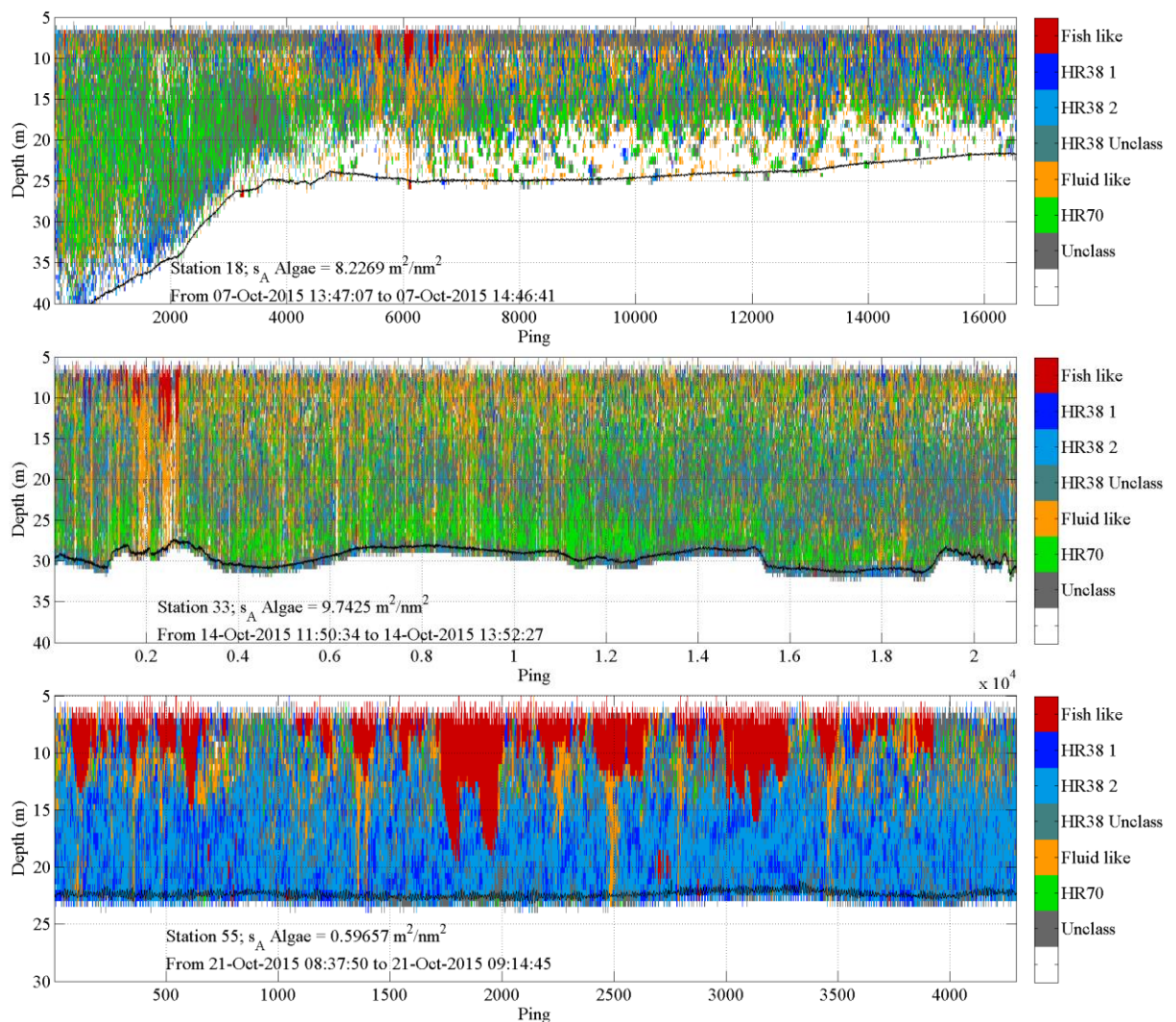


Figure 15- Acoustic groups detected in Stations 18 (upper panel) and 33 (middle panel), where pelagic algae presence was visually confirmed, and in Station 55 (lower panel), where no algae were present in the water column. The black line represents the bottom.

### Overall distribution of acoustic groups

Three-dimensional (3D) distribution of the discriminated acoustic groups shows coherent results; fish-like scatters distributed in patches throughout the water column. Dense layers of HR38<sub>1</sub> and HR38<sub>2</sub> scatters were observed over 160 m. The fluid-like scatters were mainly located below 150 m. The HR70 scatters were spare near the surface and the Unclassified scatters were distributed throughout the water column (Fig. 16). Each discriminated acoustic group was located in different areas of the multidimensional space [ $\Delta MVBS_{70-38}$ ;  $\Delta MVBS_{120-38}$ ] (Fig. 17).

A section of echogram encompassing a twilight period illustrates clear migration pattern for part of the acoustic groups (Fig. 18). Fluid-like, fish-like, HR38<sub>2</sub> and the Unclassified scatters performed vertical migration while HR38<sub>1</sub> and HR70 did not present this behavior.

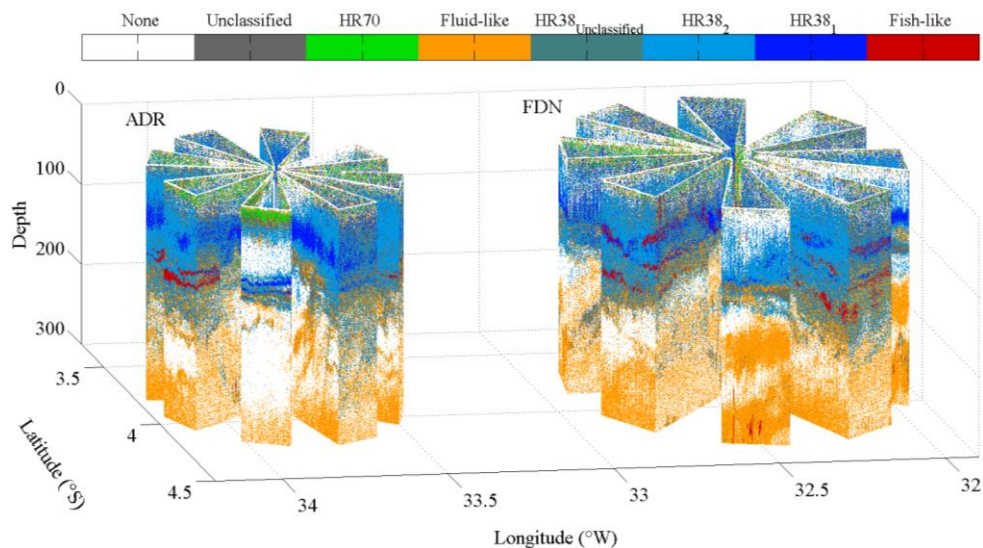


Figure 16- Three dimensional distribution of the discriminated acoustics groups.

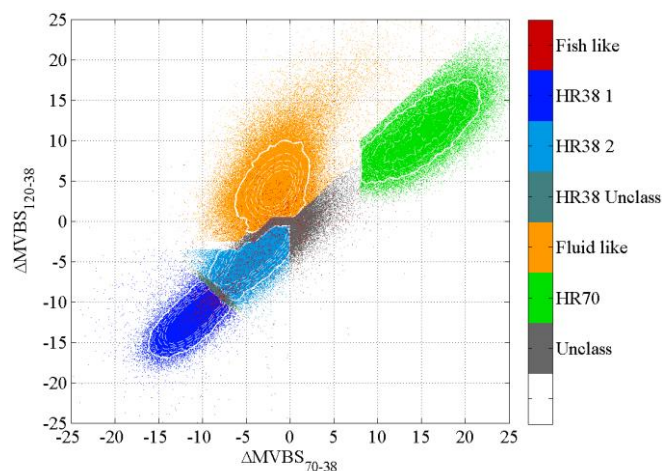


Figure 17- Spatial multifrequency distribution of the different scatters classified according their  $\Delta MVBS$ . The white lines contour areas with high density of data for each group.

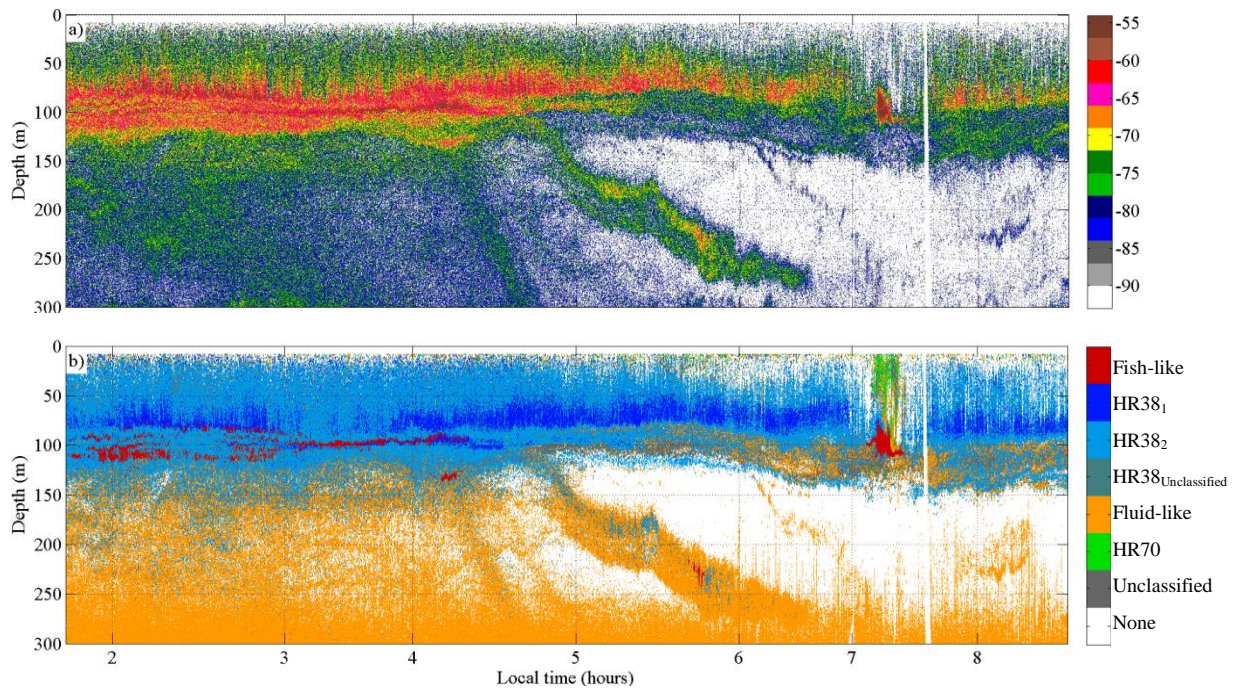


Figure 18- Comparison between (a) an echogram (38 kHz) before, and (b) after the application of the algorithm developed for multifrequency classification. This echogram encompasses night, dawn and day periods, also illustrate a pattern of downward vertical migration between 4:45 and 7:00 hours.

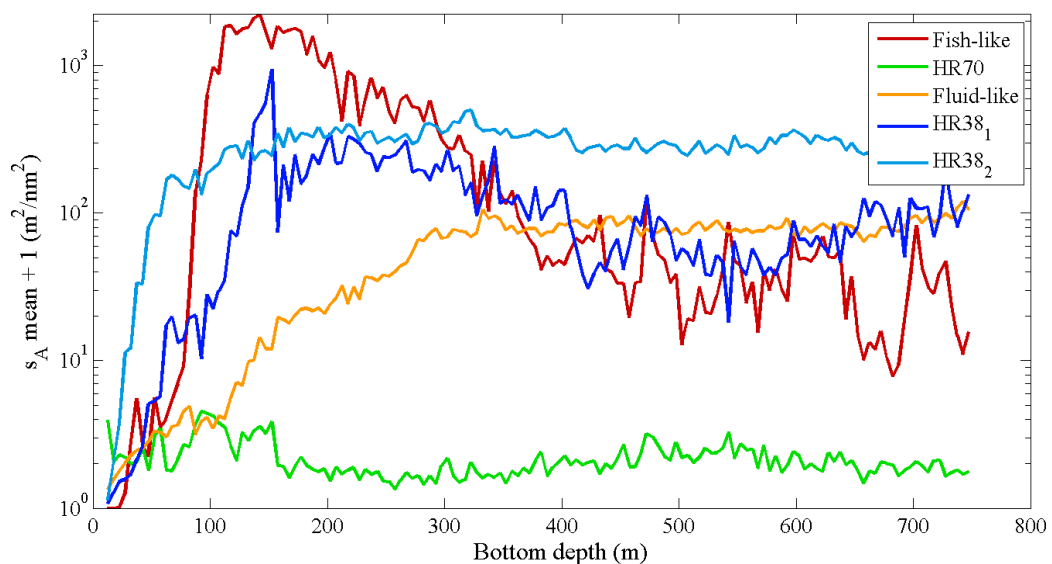


Figure 19- Distribution of the acoustic biomass ( $s_A$ ) of each acoustic group according to the bottom depth.

### Fish-like distribution

The highest acoustic biomass of fish-like echoes ( $s_A > 4000 \text{ m}^2 \text{ nm}^{-2}$ ) were observed along the shelf break of Atoll das Rocas and the Archipelago of Fernando de Noronha (Fig. 20). Indeed the fish-like group presented a clear peak of biomass at a bottom depth ranging from 100 to 200 m (Fig. 19). Farther from the islands, fish-like echoes were more abundant at night time (Fig. 20, for the diel period, see Fig. 1). The vertical distribution of fish-like echoes shows that this group was distributed throughout the water column (300 m) but with clear diel differences. Fish-like  $s_A$  was significantly higher during the night than during the day (day: 0.88, night: 1.79 y,  $p = 0.000$ ). During the day, fish-like echoes were rather evenly distributed in the water column but presented two maximums, one at 70 - 110 m corresponding to the shelf-break, the second at 180-190 m in ADR and 250-260 in FDN. During the night, the most of fish-like echoes were concentrated above 150 m (Fig. 21).

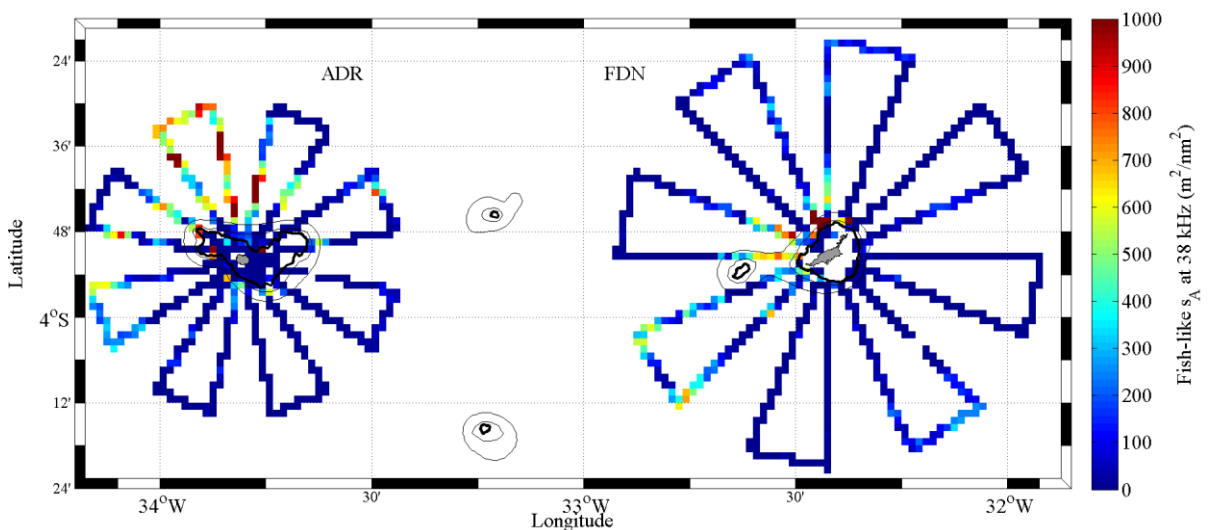


Figure 20- Spatial distribution of fish-like  $s_A$  at 38 kHz integrated in the first 300 m around ADR and FDN, averaged in grid size of  $1 \text{ nm} \times 1 \text{ nm}$ . Bottom depth contour lines in black for 100 (thick line), 300 and 500 m.

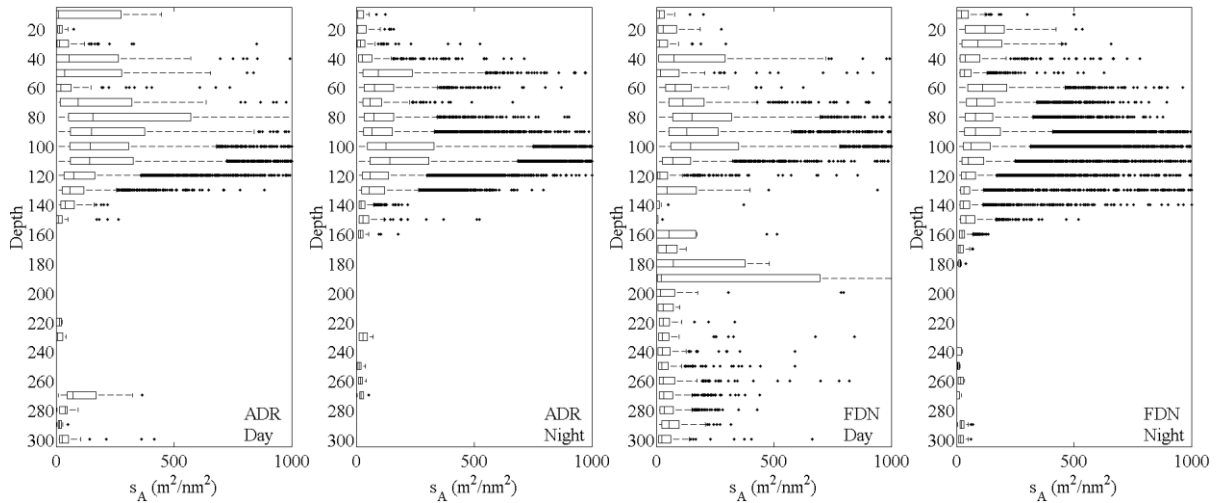


Figure 21- Vertical distribution of Fish-like  $s_A$  values at 38 kHz greater than zero around ADR and FDN, averaged in 10 m layers.

### HR70 distribution

Spatially, the HR70 group was more abundant in the western part of FDN and ADR, in particular in the south-southwest (SSW) of ADR (Fig. 22). The biomass was slightly higher at bottom depth lower than 200 m with  $s_A$  values higher than  $5 \text{ m}^2 \text{ nm}^{-2}$  (Fig. 19). Significant diel difference were observed in HR70  $s_A$  (day: 0.34, night: 0.18,  $p = 0.000$ ). Vertically, HR70 presented an overall decreasing trend from the surface up to 100 m (Fig. 23).

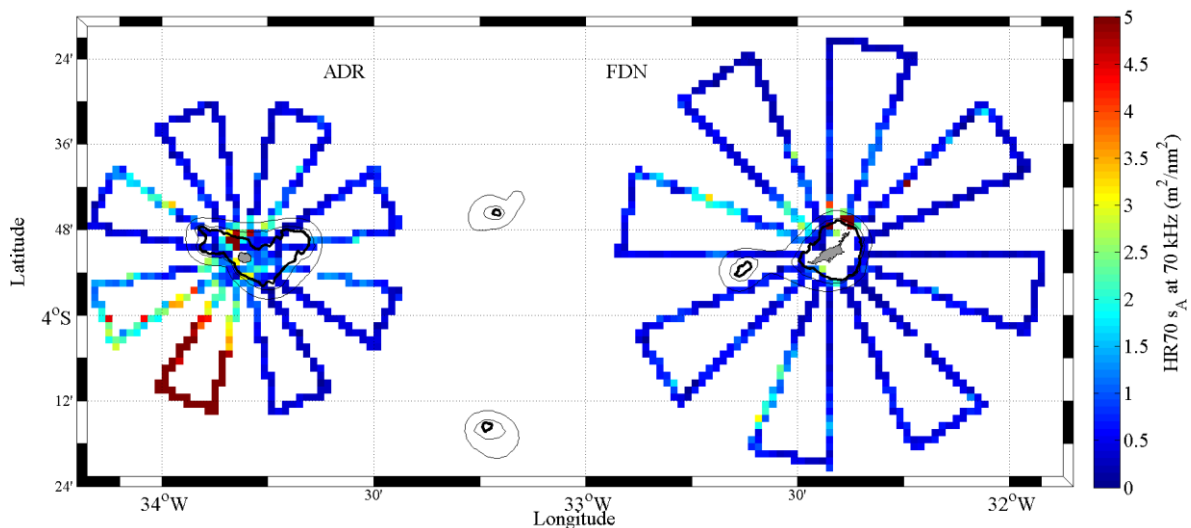


Figure 22- Spatial distribution of HR70  $s_A$  at 70 kHz integrated in the first 100 m around ADR and FDN, averaged in grid size of  $1 \text{ nm} \times 1 \text{ nm}$ . Bottom depth contour lines in black for 100 (thick line), 300 and 500 m.

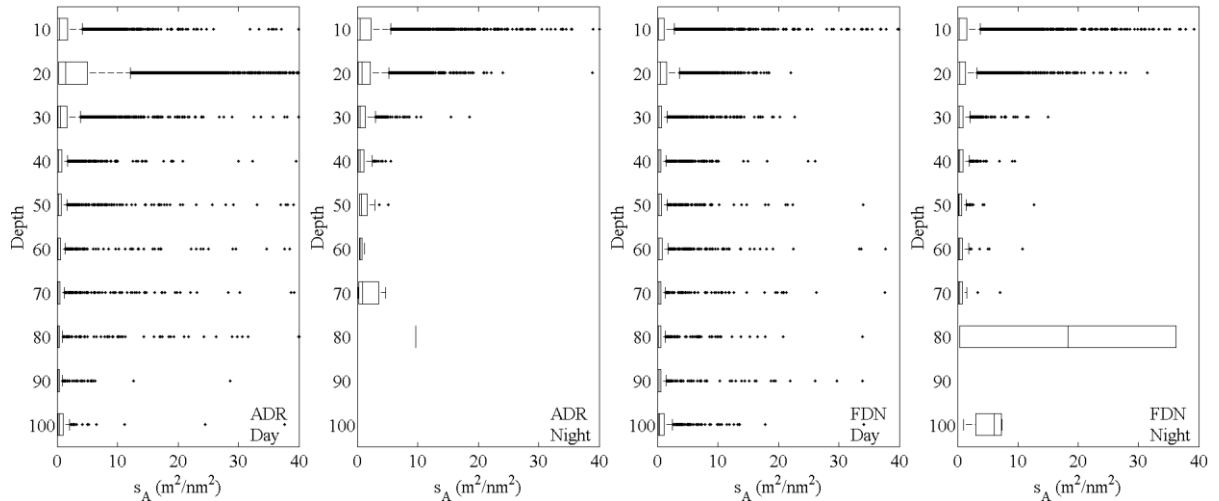


Figure 23- Vertical distribution of HR70  $s_A$  values at 70 kHz greater than zero around ADR and FDN, averaged in layers each 10 m.

### Fluid-like distribution

The fluid-like group was distributed throughout the studied area (Fig. 24), with  $s_A$  higher around FDN (over  $250 \text{ m}^2 \text{ nm}^{-2}$ ) than ADR (less than  $150 \text{ m}^2 \text{ nm}^{-2}$ ). The fluid-like biomass was low over the shelf and increased after the shelf break (Fig. 19). A clear diel pattern was observed ADR with fluid-like  $s_A$  significantly higher during the night than during the day (day: 0.80, night: 2.01,  $p = 0.000$ ). This diel pattern was also clear when looking at the vertical fluid-like distribution (Fig 25) of fluid-like. Higher biomass was observed below 200 m during the day and a pick of abundance appeared at night, at 100-180 m.

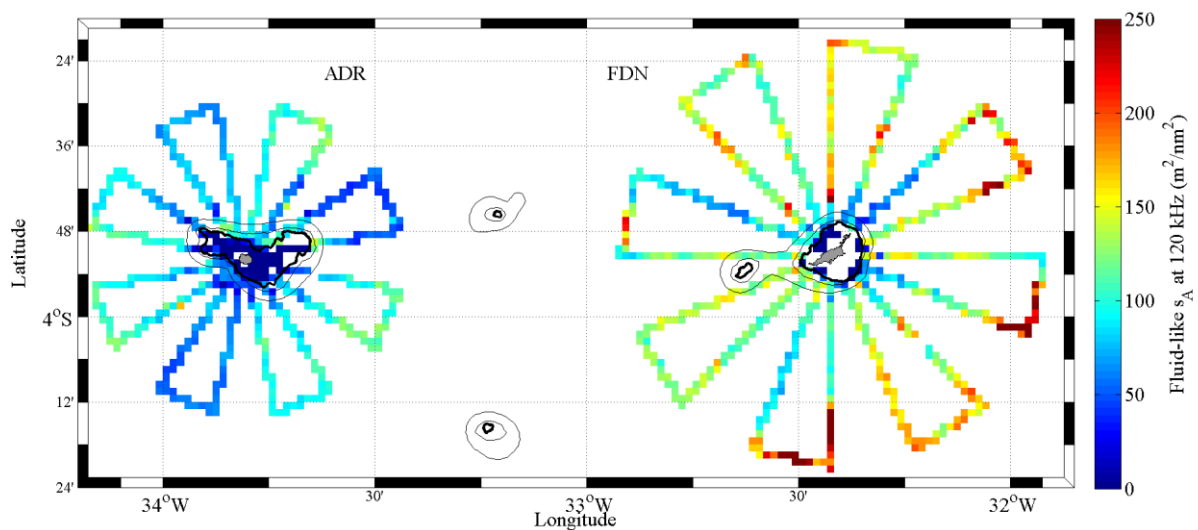


Figure 24- Spatial distribution of fluid-like  $s_A$  at 120 kHz integrated in the first 300 m around ADR and FDN, averaged in grid size of  $1 \text{ nm} \times 1 \text{ nm}$ . Bottom depth contour lines in black for 100 (thick line), 300 and 500 m.



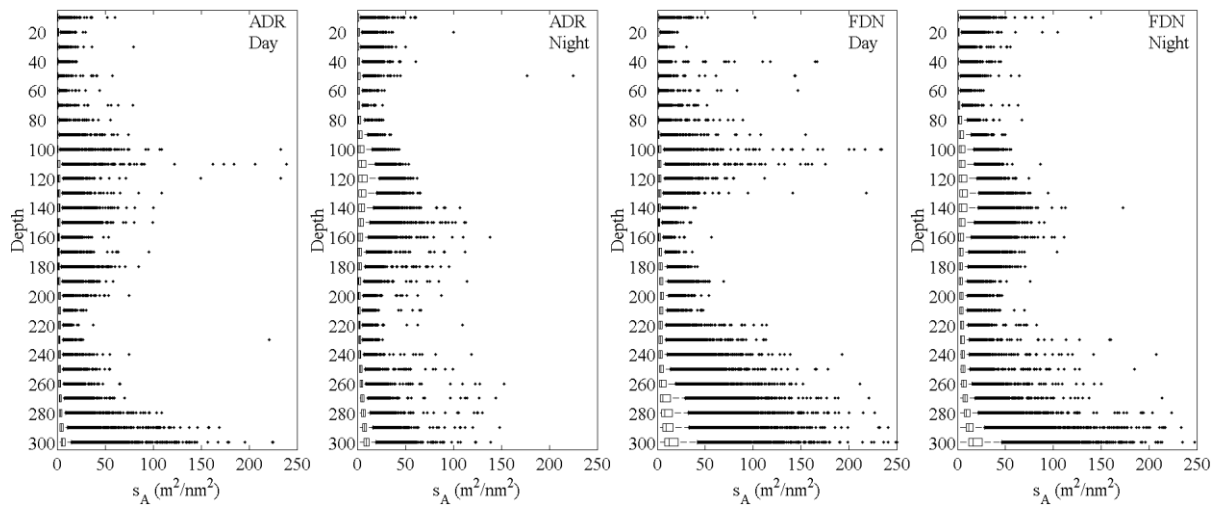


Figure 25- Vertical distribution of fluid-like  $s_A$  values at 120 kHz greater than zero around ADR and FDN, averaged in layers each 10 m.

### HR38<sub>1</sub> distribution

HR38<sub>1</sub> were more abundant in the west side of FDN and the north-northwest side of ADR, with  $s_A$  values over  $1000 \text{ m}^2 \text{ nm}^{-2}$  (Fig. 26). HR38<sub>1</sub>  $s_A$  was low over the shelf and increased markedly after the shelf-break (Fig. 19). Significant diel difference in HR38<sub>1</sub>  $s_A$  was observed between day and night (day: 1.86, night: 2.05,  $p < 0.0001$ ). Indeed this group presented a consistent vertical distribution picking between 70 and 110 m, independent of the diel period (Fig. 27).

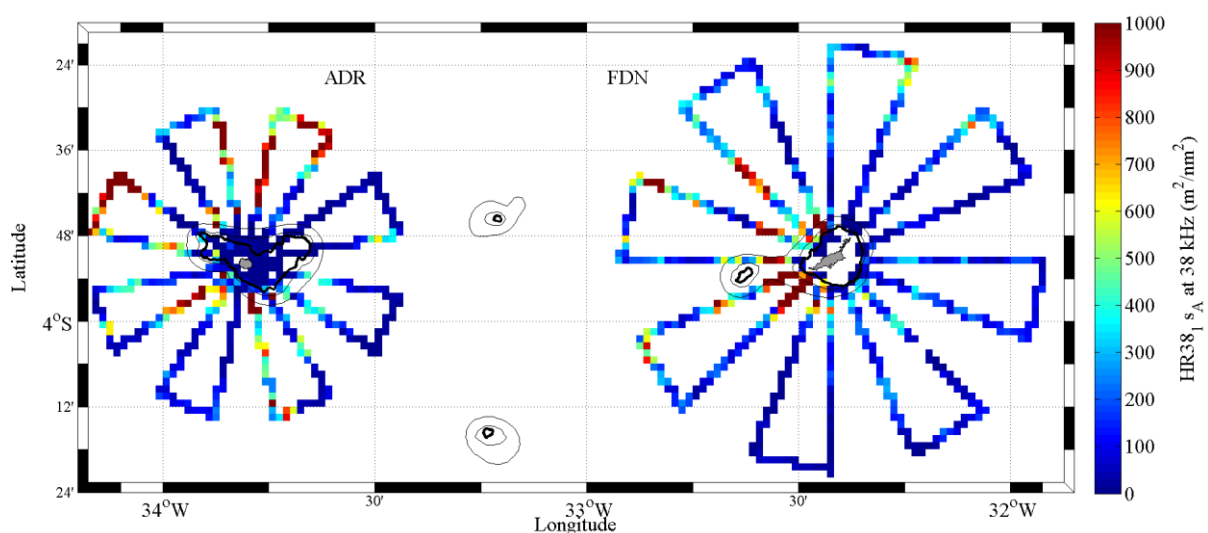


Figure 26- Spatial distribution of HR38<sub>1</sub>  $s_A$  at 38 kHz integrated in the first 300 m around ADR and FDN, averaged in grid size of  $1 \text{ nm} \times 1 \text{ nm}$ . Bottom depth contour lines in black for 100 (thick line), 300 and 500 m.

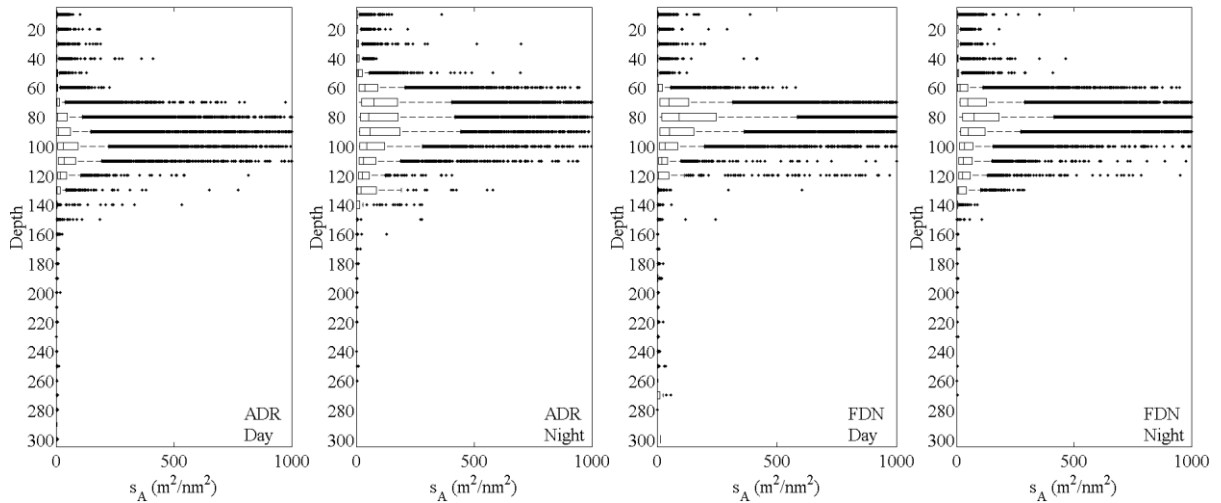


Figure 27- Vertical distribution of HR38<sub>1</sub>  $s_A$  values at 38 kHz greater than zero around ADR and FDN, averaged in layers each 10 m.

### HR38<sub>2</sub> distribution

HR38<sub>2</sub> echoes were distributed throughout the area (Fig. 28) but as for HR38<sub>1</sub> its acoustic biomass strongly increased after the shelf-break (Fig. 19). A clear diel pattern was observed with HR38<sub>2</sub>  $s_A$ , significantly higher during the night than during the day (day: 124.15, night: 516.16,  $p = 0.000$ ). Vertically, most HR38<sub>2</sub> were distributed between 90 and 120 m during the day. This range extended to 40 - 130 m during the night. Finally, a small pick of HR38<sub>2</sub> was observed during the day but disappeared at night (Fig. 29).

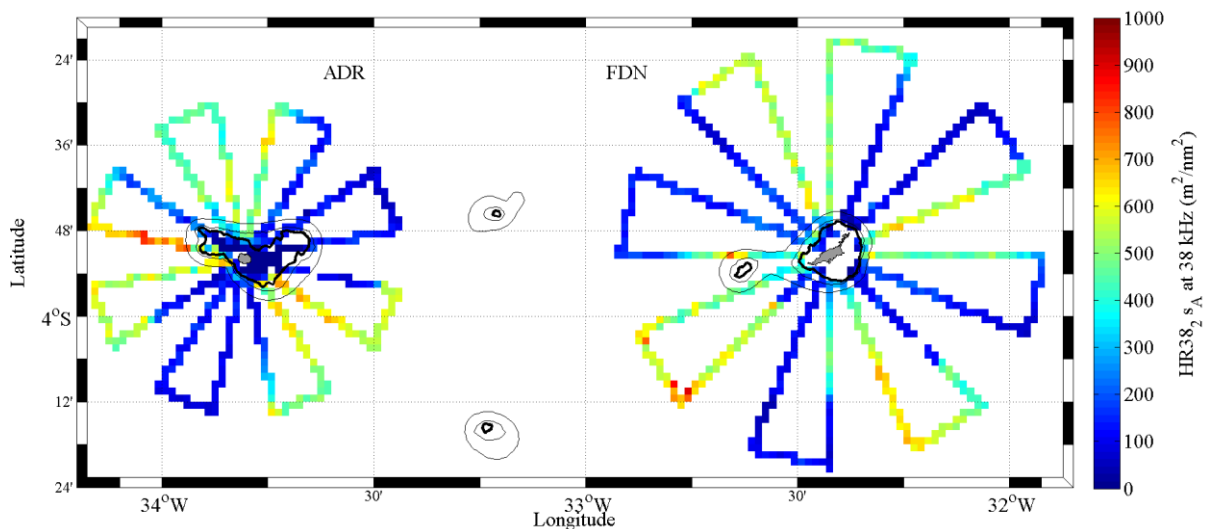


Figure 28- Spatial distribution of HR38<sub>2</sub>  $s_A$  at 38kHz integrated in the first 300 m around ADR and FDN, averaged in grid size of 1 nm  $\times$  1 nm. Bottom depth contour lines in black for 100 (thick line), 300 and 500 m.

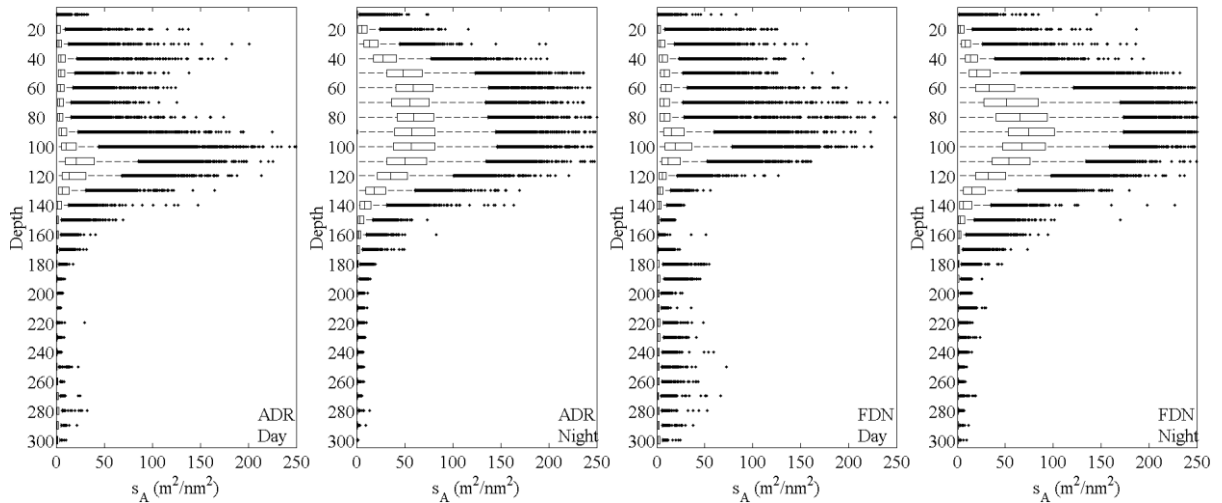


Figure 29- Vertical distribution of HR38<sub>2</sub>  $s_A$  values at 38 kHz greater than zero around ADR and FDN, averaged in layers each 10 m.

### Unclassified distribution

The group of unclassified echoes was distributed throughout with aggregations both near the shelf break and offshore (Fig. 30). However, the overall acoustic biomass was low ( $s_A < 100 \text{ m}^2 \text{ nm}^{-2}$ ). A clear diel pattern was observed with Unclassified  $s_A$ , significantly higher during the night than during the day (day: 1.27, night: 1.57,  $p = 0.000$ ). Vertically, the higher biomasses were distributed in the first 150 m (Fig. 31). The abundance of Unclassified echoes is higher in this layer during the day. However, echoes distributed below 200 m decrease in abundance during at night.

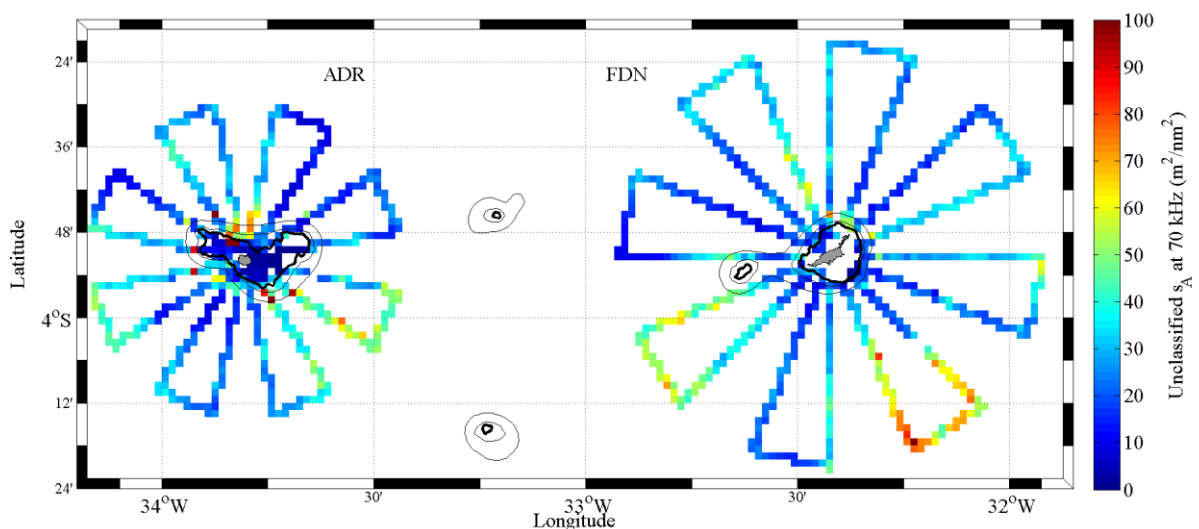


Figure 30- Spatial distribution of Unclassified  $s_A$  at 70 kHz integrated in the first 300 m around ADR and FDN, averaged in grid size of  $1 \text{ nm} \times 1 \text{ nm}$ . Bottom depth contour lines in black for 100 (thick line), 300 and 500 m.

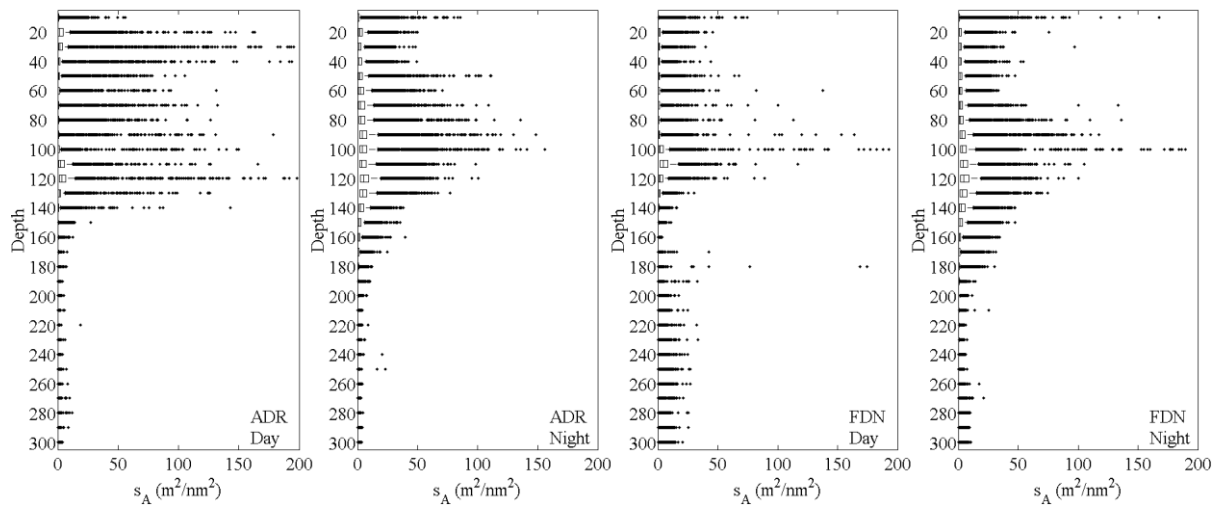


Figure 31- Vertical distribution of Unclassified  $s_A$  values at 70 kHz greater than zero around ADR and FDN, averaged in layers each 10 m.

### Discussion

The multifrequency algorithm developed in this work appears to efficiently discriminate a variety of acoustic scatters in a high biodiversity tropical system. The characteristics of the acoustic groups are consistent with what is known about their patterns of distribution. Additionally, the settings and thresholds used are consistent with previous works that used multifrequency analyses (KORNELIUSSEN and ONA, 2002; KORNELIUSSEN et al., 2009; DE ROBERTIS et al., 2010; WOILLETZ et al., 2012; SATO et al., 2015). The discussion will focus (i) on the validation of the results, (ii) on the characteristics of the proposed algorithm, and (iii) on the spatiotemporal patterns of distribution of the defined acoustic groups.

### Validation

Validating acoustic group on the basis of *in situ* catches is not an easy task since both acoustic classification and catch composition present different patterns of selectivity. For instance weak acoustic echoes corresponding to a given group (e.g., zooplankton) can be masked by a less abundant but strongest scatter (e.g., gelatinous) in the same sampled volume (LAVERY et al., 2007). On the same way catch composition depends on trawl efficiency and some groups can be overestimated when compared with others (DORAY et al., 2010).

Our results show that fish-like acoustic biomasses and fish catches were significantly correlated. Such result does not ensure that the estimated acoustic biomass represents exactly the biological biomass. Indeed the fishing gear can be visually detected by fish that can avoid and escape from the net according their swimming capabilities (KILLEN et al., 2015). The

vessel by itself generates physical disturbances that contribute to fish avoiding (SORIA et al., 1996). For these reasons only data from trawls performed at night were used for the validation. Fish could easily avoid the trawl used in this study since it has only 4 mm cod-end mesh and was towed at low speed (~2 knots). It is only at night, when myctophids were densely distributed that catches could be more representative of the actual communities.

Weak but significant positive correlation was observed between HR38 and captures of gelatinous and fish larvae. This low correlation could be due to a variety of factors. First the *in situ* sampling of gelatinous was not performed in a full quantitative way. Gelatinous were globally underestimated in the catches. Furthermore gear efficiency can affect gelatinous catches (DORAY et al., 2010). Finally, more work is still needed to determine the species corresponding to the HR38<sub>1</sub> compared to HR38<sub>2</sub>. Preliminary *in situ* observations indicate that HR38<sub>1</sub> corresponds mainly to salps and HR38<sub>2</sub> to jellyfish.

This work is the first to characterize pelagic algae using multifrequency acoustic. Several species of algae, mainly from Rhodophyceae and Chlorophyceae family are known to occur in the sampled area (VILLAÇA et al., 2002; FIGUEIREDO et al., 2008). The qualitative validation performed shows a correspondence between algae presence and acoustic biomass of HR70 scatters. HR70 showed high biomass in stations where pelagic algae have been observed and low biomass in the station where no pelagic algae have been detected.

Unfortunately, fluid-like group could not be validated at this stage. Indeed more work is needed on the *in situ* samples of crustaceans and gelatinous before to be able to compare them with the acoustic data. Such validation is not easy since zooplankton sampling using zooplankton nets has several limitations (related for instance to the zooplankton patchiness) which make difficult their comparison with acoustic data (GREENLAW, 1979). For future studies, the use of distribution patterns about species related with fluid-like and HR38 could be complemented by the quantitative validation of these groups (BALLÓN et al., 2011).

### **The algorithm**

In the algorithm, the fish-like group was defined using the sum of three pairs of frequencies (+MVBS<sub>38+70</sub>, +MVBS<sub>38+120</sub> and +MVBS<sub>70+120</sub>) and two pairs of frequency differences ( $\Delta$ MVBS<sub>70-38</sub> +  $\Delta$ MVBS<sub>120-38</sub>). So far, most studies used algorithms based only on  $\Delta$ MVBS to discriminate fish. BALLÓN et al. (2011) and LEZAMA-OCHOA et al. (2014) used the combination of +MVBS and  $\Delta$ MVBS, but their study was based on only two frequencies (38 and 120 kHz). In this study, three frequencies (38, 70, 120) were used, hence

the number of bi-frequencies pairs increased from one to three. This allowed the improvement of the discrimination of fish-like echoes. Indeed, other groups of echoes, e.g. gas-bearing gelatinous, may be highly resonant at one frequency making a given (or the total) sum of frequencies high, even if the results is related to one frequency, only. More generally, the combination of +MVBS and  $\Delta$ MVBS applied to three frequencies or more open interesting perspectives to further discriminate between fish groups. Except for FERNANDES et al. (2005), BALLÓN et al., (2011) e LEZAMA-OCHOA et al., (2014) that used such combination, all the available studies that discriminated a variety of fish groups, were based only on  $\Delta$ MVBS (KLOSER et al., 2002; DE ROBERTIS et al., 2010; WOILLEZ et al., 2012).

Once extracted the fish-like scatters from the acoustic data, echoes with characteristics corresponding to algae (HR70) were discriminated. Preliminary results showed that these scatters are highly resonant at 70 kHz (LEBOURGÉS-DHAUSSY et al., 2016). This study is the first to use acoustic methods to detect ‘pelagic algae’. So far, acoustic was only applied to detect benthonic algae. For such purpose, most methods are based on seabed acoustic classification and only one frequency is used (e.g. ANDERSON, 2002; MIELCK et al., 2014; PUHR et al., 2014). In our case, to improve algae discrimination five out of the six possible pairs of  $\Delta$ MVBS when using four frequencies ( $\Delta$ MVBS<sub>120-70</sub>,  $\Delta$ MVBS<sub>200-70</sub>,  $\Delta$ MVBS<sub>200-120</sub>,  $\Delta$ MVBS<sub>70-38</sub> and  $\Delta$ MVBS<sub>200-38</sub>) were used. Our results revealed that pelagic algae scatters have a multifrequency pattern with a minimum acoustic response at 38 kHz (~ -89 dB), a pick at 70 kHz (~ -74 dB), and a decreasing at 120 and 200 kHz (~-78 and ~-83 dB respectively). Interestingly, the multifrequency response for individual algae (TS) is different: 38 kHz > 70 kHz > 120 kHz > 200 kHz (LEBOURGÉS-DHAUSSY et al., 2016). The reason for such difference is still puzzling. One interesting aspect is that individual algae echoes are better defined (more ‘precise’) at 38 kHz than at higher frequencies. Algae echoes seem to ‘drool’ at frequencies  $\geq 70$  kHz and to occupy more space in the echogram, which could be the cause for such contradictory results. The physical acoustic reasons for such patterns still need to be investigated.

The next group discriminated was the fluid-like, which corresponds to crustacean zooplankton (STANTON et al., 1998; KORNELIUSSEN and ONA, 2002). To extract this group, the following bi-dimensional plane was used: [ $\Delta$ MVBS<sub>70-38</sub>;  $\Delta$ MVBS<sub>120-38</sub>]. This group has higher acoustics response at 120 and 200 kHz than at lower frequencies (GREENLAW, 1979; HOLLIDAY, 1980) and was thus mainly located into the first and second quadrant in

this plane (where  $\Delta MVBS_{120-38}$  is positive); although a small part was located into the third quadrant (where  $\Delta MVBS_{120-38}$  is negative). Many other studies used the multifrequency differences ( $\Delta MVBS$ ) to characterize the fluid-like (e.g., COCHRANE et al., 1991; TREVORROW et al., 2005). The thresholds defined to discriminate this group are consistent with those studies. A characteristic of the defined fluid-like group was the presence of an important number of echoes with negative  $\Delta MVBS_{70-38}$  values. This unexpected result could be related with the shape of the size-spectra of dominant zooplankters (GREENLAW, 1979; KORNELIUSSEN and ONA, 2003; BENOIT-BIRD and LAWSON, 2016). More analyses are needed to confirm this hypothesis. According to SIMMONDS & MACLENNAN (2005), it is possible to compare the multifrequency characteristics with the plankton size spectra in different layers to improve fluid-like classification. Since a consistent zooplankton sampling was accomplished during the survey using different mesh size, this kind of analysis can be performed in the future.

To discriminate echoes with characteristics corresponding to gelatinous (HR38<sub>1</sub> and HR38<sub>2</sub> groups) the same bi-dimensional plane than for fluid-like was used: [ $\Delta MVBS_{70-38}$ ;  $\Delta MVBS_{120-38}$ ]. On this plane, the gelatinous groups that are resonant at 38 kHz are located into third quadrant, where  $\Delta MVBS_{70-38}$  and  $\Delta MVBS_{120-38}$  are negatives (from  $\sim -20$  to 0 dB). The thresholds defined to discriminate these groups are consistent with previous studies. BRIERLEY et al. (2004) showed that the TS of two species of jellyfish (*Chrysaora hysoscella* and *Aequorea aequorea*) were -6 to -3 dB higher at 38 than 120 kHz. WOILLEZ et al. (2012) applied a generalized Gaussian mixture model on three frequencies (18, 38 and 120 kHz). They discriminated a group of scatters highly resonant at 18 kHz named “high 18” that they associated to jellyfish, fish larvae and siphonophores. This group also presented a higher acoustic response at 38 kHz than 120 kHz with negative difference of 2 to 15 dB. By taking advantage of the potential of discrimination of the three frequencies, ( $\Delta MVBS_{70-38}$  and  $\Delta MVBS_{120-38}$ ), our algorithm allowed discriminating two types of resonant scatters at 38 kHz (HR38<sub>1</sub> and HR38<sub>2</sub>). These groups correspond to different functional group in terms of species composition (e.g. salps for HR38<sub>1</sub>) and patterns of distribution. Finally, to ensure a robust classification among groups and reduce the overlap between scatter from HR38<sub>1</sub> and HR38<sub>2</sub> groups, an Unclassified group (HR38<sub>Unclassified</sub>) that may correspond to a mixture of the two types of gelatinous-like echoes was defined. In order to maximize the homogeneity of the acoustic group and limit the overlap between them, the 0.5% of echoes form the tail of distribution of each group (except fish-like) were separated as ‘Unclassified’. This kind of

approach ensure the robustness of the results for other groups and is classically used in acoustic studies (e.g. WOILLEZ et al., 2012).

### **Acoustic groups spatial distribution**

Our approach allowed describing the main spatiotemporal patterns of various acoustic groups along the diel cycle. It reveals a variety of spatiotemporal patterns for the different groups defined. Organisms were aggregated in patches and/or layers, and many of them performed clear diel vertical migrations (fish-like, fluid-like, HR38<sub>2</sub> and Unclassified group).

Fish-like echoes presented two different patterns. A large pick of biomass was concentrated close to the shelf break. This pattern can be related to demersal and large pelagic fish associated or concentrated close to the shelf break e.g. barracuda (*Sphyraena barracuda*) tuna (*Thunnus albacares*), wahoo (*Acantocybium solandri*), Lutjanidae (*Lutjanus* spp.) or Carangidae (*Caranx* spp.) (WEIGERT and MADUREIRA, 2011). Such pattern is well known by fishermen who concentrate their fishing effort on the shelf break (MANCINI, 2013).

The second type of fish-like echoes was distributed further offshore and performed diel vertical migration (DVM). The DVM is a known behavior for mesopelagic fish (PEARCY et al., 1977; FISHER and PEARCY, 1983). DVM can be defined as the synchronized movement of fish and zooplankton through the water column over a daily period. This is an ubiquitous phenomenon around the world, documented in marine and freshwater (BRIERLEY, 2017). Indeed, organisms that perform DVM usually ascend from meso (200 - 2000 m) to epipelagic (10 -100 m) layers at dusk, and descend back at dawn (CATUL et al., 2011). The DVM is mainly performed by fish to maintain the proximity to prey and to reduce predation from visually-cued predators. This mean that, the mesopelagic fish ascend to predate over another migrant species (e.g., euphausiids) and descend back at dawn to reduce predation from visually-cued predators (e.g. seabirds) (ROBISON, 2003; CATUL et al., 2011).

*In situ* sampling revealed that the mesopelagic fish community was dominated by Myctophidae, more specifically by species from the genera *Diaphus*, *Lepidophanes* and *Symboloporus*. These genera represented ~74% (in weigh) of Myctophidae catches during the survey (ABRAÇOS, unpublished data). These species, that dominate close to ADR and FDN, are known to perform DVM (WEIGERT and MADUREIRA, 2011; BRAGA et al., 2014). Hence, it can be assumed that the echoes from this second group can be related to the mesopelagic fish community.



This group performed DVM and, in the first 300 m, its biomass was therefore higher at night than during the day. However, the increase in fish biomass at night is not necessarily exclusively explicated by the displacement of mesopelagic fish during DVM. In a fish, the swimbladder represents 90 - 95% of the echo energy or TS (FOOTE, 1985). Fish swimbladder undergoes physiological changes during the DVM, due to the severe pressure changes (GODØ et al., 2009). Hence, when mesopelagic fish ascend, the decreasing of pressure increase the swimbladder volume, intensifying the TS (KLOSER et al., 2002; GODØ et al., 2009). In consequence, the increase in TS results in an increasing biomass in the epipelagic layer. Occurrence of inflated swimbladder in species of the genera *Diaphus* and *Lepidophanes* (dominant in the studied area) is documented off southern California (NEIGHBORS, 1992).

The HR70 group, associated to pelagic algae, presented higher values over the shelf. Benthic algae (Rhodophyceae and Chlorophyceae) have been reported in the shelf of FDN and ADR (KIKUCHI, 1999; VILLAÇA et al., 2002; FIGUEIREDO et al., 2008). The pelagic algae observed over the shelf are thus likely sections of the benthonic algae transported by currents in the pelagic layer. However, pelagic algae were also observed after the shelf break, even with lower values than over the shelf. These echoes could correspond to algae of the genus *Sargassum*, which were observed buoying in the water column during the survey (ABRAÇOS, unpublished data). In general, most pelagic algae were observed in the western side of FDN and ADR, i.e., under the flow of the SEC that flows westwards (RODRIGUES et al., 2007). Significantly more algae have been observed during the day than during the night. This pattern was not expected since algae are not supposed to perform active vertical migrations. However, if a significant change in biomass was observed, a clear change in the vertical distribution of this group was not observed. Therefore the difference observed in terms of biomass could be due to a reduced capability to observe HR70 when migrating individuals (e.g. fish-like, HR38<sub>1</sub> and HR38<sub>2</sub>) concentrated in the sub-surface layer at night, sharing the same water volume with algae (LAVERY et al., 2007).

Spatially, fluid-like acoustic biomass increased after the shelf-break. This is a classic pattern for the migrant mesopelagic crustacean community that is more abundant off the shelf-break (e.g. Ballón et al., 2011). Indeed, the vertical distribution of fluid-like was influenced by the diel cycle with significantly higher biomass during the night than during the day. The DVM in zooplankton has been documented around the world in marine and fresh waters (ROBISON, 2003; BRIERLEY, 2017). A variety of zooplankters ascend at dusk to

feed over phytoplankton and microzooplankton that occur in maximal densities in near surface waters and descend back at down to reduce predation as a defensive strategy (HAYS, 2003). Also, some zooplankton species perform DVM to reduce the risk of damage from ultraviolet radiation during the day (LEECH and WILLIAMSON, 1999).

DVM behavior was expected since the fluid-like group was dominated by Euphausiids (*Euphausia spp.*) (ABRAÇOS, unpublished data) that are known to distribute offshore and perform diel vertical migration (HAYS, 2003). The nighttime increment of biomass was not clear at depth less than 100 m. As in the case of HR70, this can be related to the concentration of stronger acoustic scatters (e.g. Fish-like, HR38<sub>1</sub> and HR38<sub>2</sub>) in sub-surface by DVM, that masked and reduced the capability to observe the fluid like scatters (LAVERY et al., 2007). From all acoustic groups described, HR38<sub>1</sub> presented the highest acoustic biomass.  $S_A$  over 1000 m<sup>2</sup> nm<sup>-2</sup> were detected around FDN and ADR. Preliminary results from *in situ* sampling performed during the survey indicate that this group was likely related to tunicates (salps) that were highly abundant over the thermocline (from ~30 to ~90-100 m). This group did not perform clear diel vertical migration. The biomass was higher at night, but this pattern is likely more a stochastic effect of the spatial sampling strategy along the diel cycle (e.g. higher nighttime sampling effort in area of concentration), than an actual behavior patterns of these organisms. Indeed the vertical distribution of this group is consistent between day and night. On the opposite hand, the HR38<sub>2</sub> echoes performed clear vertical migration and can be related with other types of gelatinous, in particular cnidarian (ABRAÇOS, unpublished data) that are known to perform diel vertical migration (e.g. BRIERLEY et al., 2004). Finally, the Unclassified group presented spatiotemporal patterns of distribution similar to HR38<sub>2</sub> and fluid-like (clear vertical migration and higher distribution off the shelf-break). It suggests that Unclassified group is therefore mainly composed by a mixture of another acoustic groups.

In conclusion, the application of this original multifrequency acoustic method opens new possibilities to observe the ecosystem in three-dimensions. For instance, its application revealed the presence of a dense layer of gelatinous on the epipelagic layer and bounded by the thermocline, which have never been documented. The consistency of this layer around the oceanic islands calls for more studies about the role of gelatinous on ecosystem structure and function. In the same way, the developed methods allowed to observe, for the first time, the presence of pelagic algae in the water column. This achievement will permit characterizing the spatiotemporal patterns of distribution and abundance in this and other ecosystems.

More generally, this algorithm that has promising capabilities and already revealed unknown ecosystems features, can be easily adapted and applied to any pelagic ecosystem (tropical or not). The capability to discriminate simultaneously, with a high spatiotemporal resolution a variety of acoustic communities, should foster ecological studies, improve the assessment of marine resources and feed ecosystem models.

## References

- ANDERSON, J. T.; HOLLIDAY, D. V.; KLOSER, R. J.; REID, D. G.; SIMRAD, Y. Acoustic seabed classification: current practice and future directions. **ICES Journal of Marine Science**, v. 65, p. 1004–1011, 2008.
- BALLÓN, M.; BERTRAND, A.; LEBOURGES-DHAUSSY, A.; GUTIÉRREZ, M.; AYÓN, P.; GRADOS, D.; GERLOTTO, F. Is there enough zooplankton to feed forage fish populations off Peru? An acoustic (positive) answer. **Progress in Oceanography**, v. 91, p. 360–381, 2011.
- BENOIT-BIRD, K. J.; LAWSON, G. L. Ecological Insights from Pelagic Habitats Acquired Using Active Acoustic Techniques. **Review in Advance**, p. 1–28, 2016.
- BERTRAND, A.; GRADOS, D.; COLAS, F.; BERTRAND, S.; CAPET, X.; CHAIGNEAU, A.; VARGAS, G.; MOUSSEIGNE, A.; FABLET, R. Broad impacts of fine-scale dynamics on seascape structure from zooplankton to seabirds. **Nature Communications**, v. 5, 2014.
- BRAGA, C.; COSTA, P. A. S.; MARTINS, A. S.; OLAVO, G.; NUNAN, G. W. Lanternfish (Myctophidae) from eastern Brazil, southwest Atlantic Ocean. **Latin American Journal of Aquatic Research**, v. 42, p. 245–257, 2014.
- BRIERLEY, A. S. Diel vertical migration. **Current Biology**, v. 24, p. R1074–R1076, 2017.
- BRIERLEY, A. S.; AXELSEN, B. E.; BOYER, D. C.; LYNAM, C. P.; DIDCOCK, C. A.; BOYER, H. J.; SPARKS, C. A. J.; PURCELL, J. E.; GIBBONS, M. J. Single-target echo detections of jellyfish. **ICES Journal of Marine Science**, v. 61, p. 383–393, 2004.
- BRIERLEY, A. S.; AXELSEN, B. E.; BUECHER, E.; SPARKS, C. A. J.; BOYER, H.; GIBBONS, M. J. Acoustic observations of jellyfish in the Namibian Benguela. **Marine Ecology Progress Series**, v. 210, p. 55–66, 2001.
- CATUL, V.; GAUNS, M.; KARUPPASAMY, P. K. A review on mesopelagic fishes belonging to family Myctophidae. **Reviews in Fish Biology and Fisheries**, v. 21, p. 339–354, 2011.
- COCHRANE, N. A.; SAMEOTO, D.; HERMAN, A. W.; NEILSON, J. Multiple-frequency

VARGAS, G. O uso da acústica multifrequência na caracterização das comunidades pelágicas em ilhas oceâni... acoustic backscattering and zooplankton aggregations in the inner Scotian Shelf basins. **Canadian Journal of Fisheries and Aquatic Sciences**, v. 48, p. 340–355, 1991.

DE ROBERTIS, A.; HIGGINBOTTOM, I. A post-processing technique to estimate the signal-to-noise ratio and remove echosounder background noise. **ICES Journal of Marine Science**, v. 64, p. 1282–1291, 2007.

DE ROBERTIS, A.; MCKELVEY, D. R.; RESSLER, P. H. Development and application of an empirical multifrequency method for backscatter classification. **Canadian Journal of Fisheries and Aquatic Sciences**, v. 67, p. 1459–1474, 2010.

DEMER, D. A.; CONTI, S. G. New target-strength model indicates more krill in the Southern Ocean. **ICES Journal of Marine Science**, v. 62, p. 25–32, 2005.

DOMINGUEZ, P. S. A pesca e o conhecimento local dos pescadores artesanais de Fernando de Noronha - PE. 2014. 69p. **Dissertação (Mestrado)** – Universidade Santa Cecília, São Paulo.

DORAY, M.; MAHÉVAS, S.; TRENKEL, V. M. Estimating gear efficiency in a combined acoustic and trawl survey, with reference to the spatial distribution of demersal fish. **ICES Journal of Marine Science**, v. 67, p. 668–676, 2010.

FERNANDES, P. G.; KORNELIUSSEN, R. J.; LEBOURGES-DHAUSSY, A.; MASSÉ, J.; IGLESIAS, M.; DINER, N.; ONA, E. Species Identification Methods From Acoustic Multi-frequency Information The SIMFAMI project: Species identification methods from acoustic multi-frequency information. **Final report to the EC. Q5RS-2001-02054**. 2005. 500p.

FIGUEIREDO, A. M. D. O.; HORTA, P. A.; PEDRINI, A. D. G.; NUNES, J. M. de C. BENTHIC MARINE ALGAE OF THE CORAL REEFS OF BRAZIL: A LITERATURE REVIEW. **Oecologia brasiliensis**, v. 12, p. 258–269, 2008.

FISHER, J. P.; PEARCY, W. G. Reproduction, growth and feeding of the mesopelagic fish. **Marine Biology**, v. 267, p. 257–267, 1983.

FOOTE, K. G. Rather-high-frequency sound scattering by swimbladdered fish. **The Journal of the Acoustical Society of America**, v. 78, p. 688–700, 1985.

FOOTE, K. G.; KNUDSEN, H. P.; VESTNES, G.; MACLENNAN, D. N.; SIMMONDS, E. J. Calibration of acoustic instruments for fish density estimation: a practical guide. **ICES Cooperative Research Report**, p. 1–69, 1987.

GARCIA, S. .; ZERBI, A.; ALIAUME, C.; DO CHI, T.; LASSERRE, G. **The ecosystem approach to fisheries**. Issues, terminology, principles, institutional foundations, implementation and outlook. FAO Fisheries Technical Paper. No. 443. Rome, FAO. 2003.

VARGAS, G. O uso da acústica multifrequência na caracterização das comunidades pelágicas em ilhas oceâni...

71p.

GODØ, O. R.; PATEL, R.; PEDERSEN, G. Diel migration and swimbladder resonance of small fish: Some implications for analyses of multifrequency echo data. **ICES Journal of Marine Science**, v. 66, p. 1143–1148, 2009.

GREENLAW, C. Acoustical estimation of zooplankton populations. **Limnological Oceanography**, v. 24, p. 226–242, 1979.

HAYS, G. C. A review of the adaptive significance and ecosystem consequences of zooplankton diel vertical migrations. **Hydrobiologia**, v. 503, p. 163–170, 2003.

HOLLIDAY, D. V. Volume scattering strengths and zooplankton distributions at acoustic frequencies between 0.5 and 3 MHz. **The Journal of the Acoustical Society of America**, v. 67, p. 135, 1980.

KIKUCHI, R. K. P. Atol das Rocas, Litoral do Nordeste do Brasil - Único atol do Atlântico Sul Equatorial Ocidental. **Sítios Geológicos e Paleontológicos do Brasil**, v. 1, p. 379–393, 1999.

KILLEN, S. S.; NATI, J. J. H.; SUSKI, C. D. Vulnerability of individual fish to capture by trawling is influenced by capacity for anaerobic metabolism. **Proceedings. Biological sciences / The Royal Society**, v. 282, p. 20150603, 2015.

KLOSER, R. J.; RYAN, T.; SAKOV, P.; WILLIAMS, a; KOSLOW, J. a. Species identification in deep water using multiple acoustic frequencies. **Canadian Journal of Fisheries and Aquatic Sciences**, v. 59, p. 1065–1077, 2002.

KORNELIUSSEN, R. J.; HEGGELUND, Y.; ELIASSEN, I. K.; JOHANSEN, G. O. Acoustic species identification of schooling fish. **ICES Journal of Marine Science**, v. 66, p. 1111–1118, 2009.

KORNELIUSSEN, R. J.; HEGGELUND, Y.; MACAULAY, G. J.; PATEL, D.; JOHNSON, E.; ELIASSEN, I. K. Acoustic identification of marine species using a feature library. **Methods in Oceanography**, v. 17, p. 187–205, 2016.

KORNELIUSSEN, R. J.; ONA, E. An operational system for processing and visualizing multi-frequency acoustic data. **ICES Journal of Marine Science**, v. 59, p. 293–313, 2002.

KORNELIUSSEN, R. J.; ONA, E. Synthetic echograms generated from the relative frequency response. **ICES Journal of Marine Science**, v. 60, p. 636–640, 2003.

LIVERY, A. C.; WIEBE, P. H.; STANTON, T. K.; LAWSON, G. L.; BENFIELD, M. C.; COPLEY, N. Determining dominant scatterers of sound in mixed zooplankton. 2007.

LEBOURGUES-DHAUSSY, A.; ROUDAUT, G.; MONTENEGRO, A.; BERTRAND, A.

VARGAS, G. O uso da acústica multifrequência na caracterização das comunidades pelágicas em ilhas oceâni...

When algae sound fishy. In: ICES - Fisheries Acoustic Science and Technology Working Group, Vigo-Spain. 2016.

LEECH, D. M.; WILLIAMSON, C. E. In situ exposure to ultraviolet radiation alters the depth distribution of *Daphnia*. **Limnological Oceanography**, v. 46, p. 416–419, 1999.

LEZAMA-OCHOA, A.; IRIGOIEN, X.; CHAIGNEAU, A.; QUIROZ, Z.; LEBOURGES-DHAUSSY, A.; BERTRAND, A. Acoustics reveals the presence of a macrozooplankton biocline in the bay of Biscay in response to hydrological conditions and predator-prey relationships. **PLoS ONE**, v. 9, p. e88054, 2014.

MACLENNAN, D. N.; FERNANDES, P. G.; DALEN, J. A consistent approach to definitions and symbols in fisheries acoustics. **ICES Journal of Marine Science**, v. 59, p. 365–369, 2002.

MANCINI, P. Relações trófica de aves marinhas tropicais em ilhas oceânicas do Brasil. 2013. 191p. **Tese (Doutorado)** - Universidade Federal do Rio Grande - FURG, Rio Grande.

MILOSLAVICH, P.; KLEIN, E.; DÍAZ, J. M.; HERNÁNDEZ, C. E.; BIGATTI, G.; CAMPOS, L.; ARTIGAS, F.; CASTILLO, J.; PENCHASZADEH, P. E.; NEILL, P. E.; CARRANZA, A.; RETANA, M. V.; DÍAZ DE ASTARLOA, J. M.; LEWIS, M.; YORIO, P.; PIRIZ, M. L.; RODRÍGUEZ, D.; VALENTIN, Y. Y.; GAMBOA, L.; MARTÍN, A. Marine biodiversity in the Atlantic and Pacific coasts of South America: Knowledge and gaps. **PLoS ONE**, v. 6, p. e14631, 2011.

NEIGHBORS, M. A. Occurrence of inflated swimbladders in five species of lanternfishes (family Myctophidae) from waters off southern California. **Marine Biology**, v. 363, p. 355–363, 1992.

PEARCY, W. G.; KRYGIER, E. E.; MESECAR, R.; RAMSEY, F. Vertical distribution and migration of oceanic micronekton off Oregon. **Deep Sea Research**, v. 24, p. 223–245, 1977.

PEREIRA, J.; GABIOUX, M.; MARTA-ALMEIDA, M.; CIRANO, M.; PAIVA, A. M.; AGUIAR, A. L. The bifurcation of the Western Boundary Current System of the South Atlantic Ocean. **Revista Brasileira de Geofísica**, v. 32, p. 241–257, 2014.

ROBISON, B. H. What drives the diel vertical migrations of Antarctic midwater fish? **Journal of the Marine Biological Association of the UK**, v. 83, p. 639–642, 2003.

RODRIGUES, R. R.; ROTHSTEIN, L. M.; WIMBUSH, M. Seasonal Variability of the South Equatorial Current Bifurcation in the Atlantic Ocean : **Journal of Physical Oceanography**, v. 37, p. 16–30, 2007.

RYAN, T. E.; DOWNIE, R. A.; KLOSER, R. J.; KEITH, G. Reducing bias due to noise and

VARGAS, G. O uso da acústica multifrequência na caracterização das comunidades pelágicas em ilhas oceâni...  
attenuation in open-ocean echo integration data. **ICES Journal of Marine Science**, v. 72, p. 2482–2493, 2015.

SATO, M.; HORNE, J. K.; PARKER-STETTER, S. L.; KEISTER, J. E. Acoustic classification of coexisting taxa in a coastal ecosystem. **Fisheries Research**, v. 172, p. 130–136, 2015.

SERAFINI, T. Z.; FRANÇA, G. B. De; ANDRIGUETTO-FILHO, J. M. Ilhas oceânicas brasileiras: biodiversidade conhecida e sua relação com o histórico de uso e ocupação humana. **Revista da Gestão Costeira Integrada**, v. 10, p. 281–301, 2010.

SIMMONDS, J.; MACLENNAN, D. **Fisheries acoustics: theory and practice**. 2nd. ed., 2005. 325p.

SORIA, M.; FRÉON, P.; GERLOTTO, F. Analysis of vessel influence on spatial behaviour of fish schools using a multi-beam sonar and consequences for biomass estimates by echosounder. **ICES Journal of Marine Science**, v. 53, p. 453–458, 1996.

STANTON, T. K.; CHU, D. Review and recommendations for the modelling of acoustic scattering by fluid-like elongated zooplankton : euphausiids and copepods. **ICES Journal of Marine Science**, v. 57, p. 793–807, 2000.

STANTON, T. K.; CHU, D.; WIEBE, P. H. Sound scattering by several zooplankton groups. II. Scattering models. **The Journal of the Acoustical Society of America**, v. 103, p. 236–253, 1998.

STRAMMA, L.; ENGLAND, M. On the water masses and mean circulation of the South Atlantic Ocean. **JOURNAL OF GEOPHYSICAL RESEARCH**, v. 104, p. 20863–20883, 1999.

TRENKEL, V. M.; BERGER, L. A fisheries acoustic multi-frequency indicator to inform on large scale spatial patterns of aquatic pelagic ecosystems. **Ecological Indicators**, v. 30, p. 72–79, 2013.

TRENKEL, V. M.; BERGER, L.; BOURGUIGNON, S.; DORAY, M.; FABLET, R.; MASSÉ, J.; MAZAURIC, V.; PONCELET, C.; QUEMENER, G.; SCALABRIN, C.; VILLALOBOS, H. Overview of recent progress in fisheries acoustics made by Ifremer with examples from the Bay of Biscay. **Aquatic Living Resources**, v. 22, p. 433–445, 2009.

TREVORROW, M. V.; MACKAS, D. L.; BENFIELD, M. C. Comparison of multifrequency acoustic and in situ measurements of zooplankton abundances in Knight Inlet, British Columbia. **The Journal of the Acoustical Society of America**, v. 117, p. 3574, 2005.

UNESCO. **World heritage papers 45. the future of the world heritage convention for**

VARGAS, G. O uso da acústica multifrequência na caracterização das comunidades pelágicas em ilhas oceâni...

**marine conservation**, 2016. 147p.

VILLAÇA, R. C.; FONSECA, A. C.; FERRAZ, A.; MARQUES, L.; JENSEN, V.; ANDRADE, V.; KNOPPERS, B.; TEIXEIRA, V. **Projeto: “ Distribuição e aspectos ecológicos das macroalgas da Reserva Biológica do Atol das Rocas ”**. 2002.32p.

WEIGERT, S. C.; MADUREIRA, L. S. P. REGISTROS ACÚSTICOS BIOLÓGICOS DETECTADOS NA ZONA ECONÔMICA EXCLUSIVA DA REGIÃO NORDESTE DO BRASIL – UMA CLASSIFICAÇÃO EM ECOTIPOS FUNCIONAIS. **Atlântica**, v. 33, p. 15–32, 2011.

WOILLEZ, M.; RESSLER, P. H.; WILSON, C. D.; HORNE, J. K. Multifrequency species classification of acoustic-trawl survey data using semi-supervised learning with class discovery. **The Journal of the Acoustical Society of America**, v. 131, p. 184–190, 2012.



#### **4- Considerações finais**

A aplicação do algoritmo apresentou resultados coerentes em termos dos padrões de distribuição acústica e espacial de cada grupo e correlação significativa para o grupo dos peixes, apesar da complexidade da aplicação da acústica multifrequência nos ecossistemas de elevada biodiversidade. A validação qualitativa não pode ser realizada para todos os grupos. Um planejamento de amostragem apropriado para a validação de cada grupo deve ser considerado, tendo em consideração as limitações das ferramentas de amostragem e o comportamento das espécies alvo.

Os resultados amostraram uma ampla distribuição de peixes principalmente associados à quebra do talude. Em relação aos gelatinosos, registrou-se uma elevada biomassa, e a sua distribuição poderia estar relacionada às correntes na zona de estudo. O zooplâncton também apresentou uma ampla distribuição, principalmente dentro da camada mesopelágica. De forma inovadora, as algas conseguiram ser classificadas usando a acústica. Este grupo foi encontrado principalmente distribuído na coluna d'água sobre a plataforma, e dentro dos primeiros 20 m da superfície na área fora da plataforma. A migração nictimeral também foi observada e se registrou um incremento significativo da biomassa na camada epipelágica de várias comunidades como peixes, zooplâncton, alguns tipos de gelatinosos e outras não definidas.

O nosso algoritmo permite a extração de informação qualitativa (e.g., grupo de espécie) e quantitativa (e.g., biomassa acústica, profundidade, localização) de alta resolução que pode ser usada para o estudo da ecologia, monitoramento, ordenamento territorial e inclusive para alimentar modelos (e.g., Ecopath) e ser replicado para outras áreas tropicais. Entretanto, o algoritmo para classificação multifrequência desenvolvido ainda pode ser melhorado. Durante as análises dos dados observou-se a possibilidade de separar os peixes e zooplâncton em menores grupos, entretanto, os métodos de amostragem devem ser aperfeiçoados para a validação de cada novo grupo.

## ANEXOS

Anexo 1- Computational code developed in Matlab (MathWorks™, Natick, Massachusetts, USA) to apply multifrequency algorithm using cleaned acoustic data.

```
%%%%%%%%%%%%%%%%%%%%%%%%%%%%%%%%%%%%%%%%%%%%%%%%%%%%%%%%%%%%%%%%%%%%%%%%%
clear all; close all

addpath 'C:\ABRACOS\Acoustic
Data\Configurations_files\Samples_Data\HAC_toolbox'

path='C:\ABRACOS\HAC_ABRACOS\er60_MBES\ADR\CleanedHac\CleanedHac\EI_Results
\BIND\';

files=dir([path,'ADR*']);
for ii=1:length(files)

    disp([files(ii).name, ' [file:
',num2str(ii), '/',num2str(length(files)),']'])
    load([path,files(ii).name], 'transFreq', 'transDepth',...
        'depth_surface', 'depth_bottom', 'Sv_surface', 'time')

    Dmax=300;
    indD=depth_surface(1,:,1)<Dmax;
    depth_surface=depth_surface(:,indD,:);
    Sv_surface=Sv_surface(:,indD,:);

    clear Ind_surface
    Ind_surface= repmat(1:size(Sv_surface,1),size(Sv_surface,2),1)';

    clear Dmax indD
    %% To Convolution and plot

    for i=1:length(transFreq)
        Sv_surface_conv(:,:,i)=gconv(Sv_surface(:,:,i),3,3);
        gtsecho(Sv_surface_conv(:,:,i)',unique(depth_surface(:,:,i)),...
            [-93 -54],depth_bottom(:,:,i))
        title([num2str(transFreq(i)/1000),' kHz'])
    end

    % To clean extreme values
    m1=Sv_surface_conv(:,:,2)-Sv_surface_conv(:,:,1);
    m2=Sv_surface_conv(:,:,3)-Sv_surface_conv(:,:,1);
    m3=Sv_surface_conv(:,:,3)-Sv_surface_conv(:,:,2);
    tt=nanmax(Sv_surface_conv(:,:,1),Sv_surface_conv(:,:,2));
    tt=nanmax(tt,Sv_surface_conv(:,:,3));

    for i=1:length(transFreq)
        Tprovi = Sv_surface_conv(:,:,i);
        indp = abs(m1)>50 | abs(m2)>50 | abs(m3)>50 | m1==0 | m2==0 | m3==0;
        Tprovi(indp)=NaN;
        Sv_surface_conv(:,:,i)=Tprovi;
    end
    clear Tprovi indp
    %% Here we start to apply the algorithm
    % Fish and Not fishes
    disp('Separating Fish and Not Fish')
```

```

m=sum(Sv_surface_conv(:,:,1:3),3);
ms1=sum(Sv_surface_conv(:,:, [1,2]),3);
ms2=sum(Sv_surface_conv(:,:, [2,3]),3);
ms3=sum(Sv_surface_conv(:,:, [1,3]),3);
ms4=sum(Sv_surface_conv(:,:, [3,4]),3);

m1=Sv_surface_conv(:,:,2)-Sv_surface_conv(:,:,1);
m2=Sv_surface_conv(:,:,3)-Sv_surface_conv(:,:,1);
m3=Sv_surface_conv(:,:,3)-Sv_surface_conv(:,:,2);
m4=Sv_surface_conv(:,:,4)-Sv_surface_conv(:,:,1);
m5=Sv_surface_conv(:,:,4)-Sv_surface_conv(:,:,2);
m6=Sv_surface_conv(:,:,4)-Sv_surface_conv(:,:,3);

%Mask
HE_mask= ms1>-134.5 & ms2>=-135 & ms3>-134 & m1+m2>=-18;

% applying mask
HE_Sv38=gmask(Sv_surface_conv(:,:,3),HE_mask,-999);

% Conv Echo
HE_Sv38_conv=gconv(HE_Sv38,3,3);

% Fish Mask
Fish_mask=HE_Sv38_conv>-100 & tt>=-80;

for i=1:length(transFreq)
%   Fish_Sv(:,:,i)=gmask(Sv_surface(:,:,i),Fish_mask,-999);
   Fish_Sv_conv(:,:,i)=gmask(Sv_surface_conv(:,:,i),Fish_mask,-999);
   gtsecho(Fish_Sv_conv(:,:,i)',unique(depth_surface(:,:,i)),...
   [-93 -54],depth_bottom(:,:,i))
   title(['Fish like ',num2str(transFreq(i)/1000),' kHz'])
end
clear HE_mask HE_Sv38 HE_Sv38_conv
%% Working with No Fish
disp('Separating HR70')

% HR70_mask
HR70_mask = ~Fish_mask & m3<2 & m5<-2 & m6<0 & m1>8 & m4>2;

for i=1:length(transFreq)
%   HR70_Sv(:,:,i)=gmask(Sv_surface(:,:,i),HR70_mask,-999);
   HR70_Sv_conv(:,:,i)=gmask(Sv_surface_conv(:,:,i),HR70_mask,-999);
   gtsecho(HR70_Sv_conv(:,:,i)',unique(depth_surface(:,:,i)),...
   [-93 -54],depth_bottom(:,:,i))
   title(['HR70 ',num2str(transFreq(i)/1000),' kHz'])
end

WEcho_mask=~Fish_mask & ~HR70_mask;

%% Working with weak echoes (No Fish and No HR70)
disp('Separating Fluid like and HR38')

% FL Mask
X1=[-6 -5 -4 -3 -2 0.5 50 -50 -50 -6];
Y1=[-2.5 -1.5 -1.5 -0.5 0.5 0.5 50 50 -2.5 -2.5];
indFL=inpolygon(m1,m2,X1,Y1);
FL_mask=WEcho_mask & indFL;
for i=1:length(transFreq)
%   FL_Sv(:,:,i)=gmask(Sv_surface(:,:,i),FL_mask,-999);

```

```

FL_Sv_conv(:,:,i)=gmask(Sv_surface_conv(:,:,i),FL_mask,-999);
gtsecho(FL_Sv_conv(:,:,i)',unique(depth_surface(:,:,i)),...
    [-93 -54],depth_bottom(:,:,i))
title(['Fluid like ',num2str(transFreq(i)/1000),' kHz'])
end

% HR38 Mask
X2=[-6 -5 -4 -3 -2 0 0 -50 -50 -6];
Y2=[-3.5 -2.5 -2.5 -1.5 -0.5 -0.5 -50 -50 -3.5 -3.5];
indHR38=inpolygon(m1,m2,X2,Y2);
HR38_mask=WEcho_mask & indHR38;
for i=1:length(transFreq)
%     HR38_Sv(:,:,i)=gmask(Sv_surface(:,:,i),HR38_mask,-999);
    HR38_Sv_conv(:,:,i)=gmask(Sv_surface_conv(:,:,i),HR38_mask,-999);
    gtsecho(HR38_Sv_conv(:,:,i)',unique(depth_surface(:,:,i)),...
        [-93 -54],depth_bottom(:,:,i))
    title(['HR38 ',num2str(transFreq(i)/1000),' kHz'])
end

% Unclassified Mask
UC_mask=WEcho_mask & ~indFL & ~indHR38;
for i=1:length(transFreq)
%     UC_Sv(:,:,i)=gmask(Sv_surface(:,:,i),UC_mask,-999);
    UC_Sv_conv(:,:,i)=gmask(Sv_surface_conv(:,:,i),UC_mask,-999);
    gtsecho(UC_Sv_conv(:,:,i)',unique(depth_surface(:,:,i)),...
        [-93 -54],depth_bottom(:,:,i))
    title(['Unclassified ',num2str(transFreq(i)/1000),' kHz'])
end

clear X1 Y1 X2 Y2 indFL indHR38
%% Working with HR38
disp('Separating HR38_1 and Not HR38_2')

HR381_mask= m1+m2<-17.5 & HR38_mask;
for i=1:length(transFreq)
%     HR381_Sv(:,:,i)=gmask(Sv_surface(:,:,i),HR381_mask,-999);
    HR381_Sv_conv(:,:,i)=gmask(Sv_surface_conv(:,:,i),HR381_mask,-999);
    gtsecho(HR381_Sv_conv(:,:,i)',unique(depth_surface(:,:,i)),...
        [-93 -54],depth_bottom(:,:,i))
    title(['HR38_1 ',num2str(transFreq(i)/1000),' kHz'])
end

HR382_mask=m1+m2>-16.5 & HR38_mask;
for i=1:length(transFreq)
%     HR382_Sv(:,:,i)=gmask(Sv_surface(:,:,i),HR382_mask,-999);
    HR382_Sv_conv(:,:,i)=gmask(Sv_surface_conv(:,:,i),HR382_mask,-999);
    gtsecho(HR382_Sv_conv(:,:,i)',unique(depth_surface(:,:,i)),...
        [-93 -54],depth_bottom(:,:,i))
    title(['HR38_2 ',num2str(transFreq(i)/1000),' kHz'])
end

HR38U_mask=m1+m2<=-16.5 & m1+m2>=-17.5 & HR38_mask;
for i=1:length(transFreq)
%     HR38U_Sv(:,:,i)=gmask(Sv_surface(:,:,i),HR38U_mask,-999);
    HR38U_Sv_conv(:,:,i)=gmask(Sv_surface_conv(:,:,i),HR38U_mask,-999);
    gtsecho(HR38U_Sv_conv(:,:,i)',unique(depth_surface(:,:,i)),...
        [-93 -54],depth_bottom(:,:,i))
    title(['HR38_{Unclass} ',num2str(transFreq(i)/1000),' kHz'])
end

```

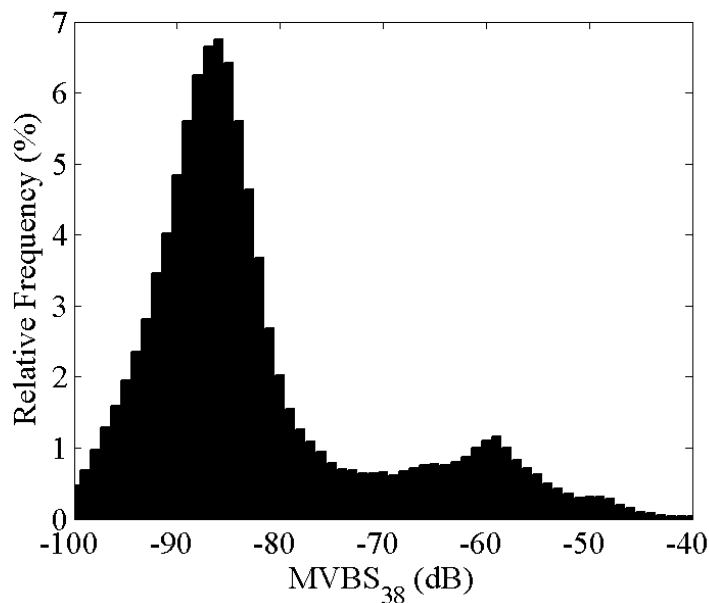
```

%% Final process
disp('Saving...')
ThrMax=-90;
Final=7*double(Fish_Sv_conv(:,:,1)>=ThrMax)+...
    6*double(HR381_Sv_conv(:,:,1)>=ThrMax)+...
    5*double(HR382_Sv_conv(:,:,1)>=ThrMax)+...
    4*double(HR38U_Sv_conv(:,:,1)>=ThrMax)+...
    3*double(FL_Sv_conv(:,:,3)>=ThrMax)+...
    2*double(HR70_Sv_conv(:,:,2)>=ThrMax)+...
    double(UC_Sv_conv(:,:,2)>=ThrMax);
Final1=Final;Final(:,:,2)=Final1;Final(:,:,3)=Final1;
Final(:,:,4)=Final1;

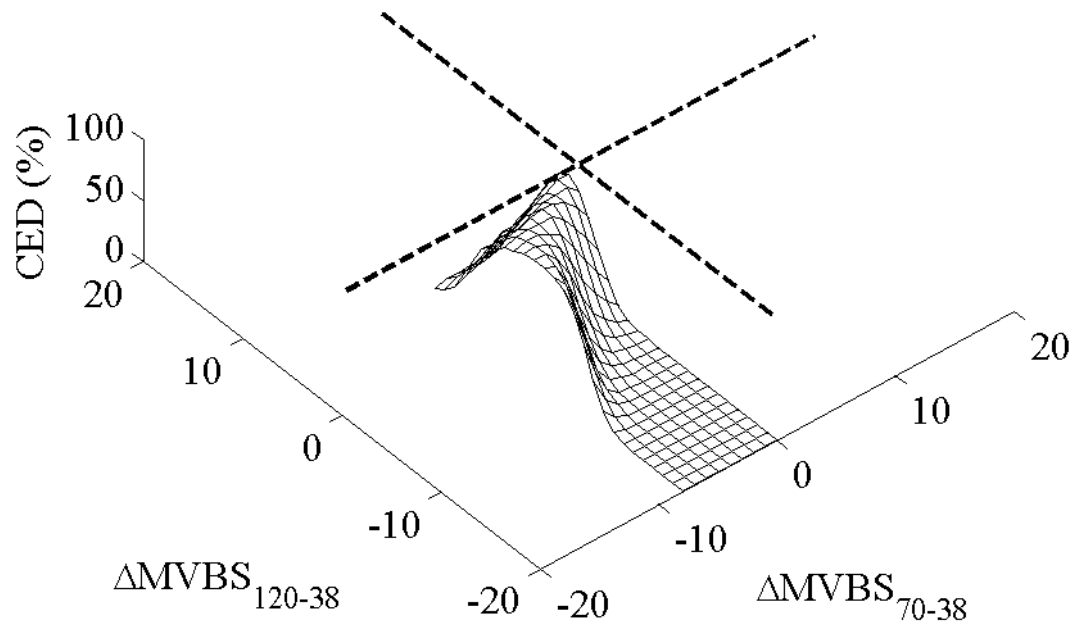
if ii<10
save([path,'Final_0000',num2str(ii),'.mat'],'Final')
end
if ii>=10 && ii<100
save([path,'Final_000',num2str(ii),'.mat'],'Final')
end
if ii>=100
save([path,'Final_00',num2str(ii),'.mat'],'Final')
end
if ii>=1000
% save([path,'Final_0',num2str(ii),'.mat'],'Final')
% end
clear Sv_surface_conv Fish_Sv_conv HR70_Sv_conv FL_Sv_conv...
    HR38_Sv_conv UC_Sv_conv HR381_Sv_conv HR382_Sv_conv HR38U_Sv_conv

close all
end
%%%%%%%%%%%%%%%%%%%%%%%%%%%%%%%%%%%%%%%%%%%%%%%%%%%%%%%%%%%%%%%%%%%%%%%%

```



Anexo 2- Histogram of MVBS values at 38 kHz of the areas containing possible fish schools.



Anexo 3- Cumulative energy difference (CED) in multidimensional space between scatters with characteristics of fluid like and high resonant at 38 kHz. The maximum CED defines the limit between groups.